IEEE Access
Multidisciplinary ⋮ Rapid Review ⋮ Open Access Journal

Received November 25, 2015, accepted December 14, 2015, date of publication December 24, 2015,
date of current version March 1, 2016.

Digital Object Identifier 10.1109/ACCESS.2015.2511558

Review of Video and Image Defogging Algorithms and Related Studies on Image Restoration and Enhancement

YONG XU[1,2], (Senior Member, IEEE), JIE WEN[1], LUNKE FEI[1], AND ZHENG ZHANG[1], (Student Member, IEEE)

[1]Bio-Computing Research Center, Shenzhen Graduate School, Harbin Institute of Technology, Shenzhen 518055, China,
[2]Key Laboratory of Network Oriented Intelligent Computation, Shenzhen 518055, China

Corresponding author: Y. Xu (yongxu@ymail.com)

This work was supported in part by the National Natural Science Foundation of China under Grant 61370163 and in part by the Shenzhen Municipal Science and Technology Innovation Council under Grant JCYJ20140904154630436.

ABSTRACT Video and images acquired by a visual system are seriously degraded under hazy and foggy weather, which will affect the detection, tracking, and recognition of targets. Thus, restoring the true scene from such a foggy video or image is of significance. The main goal of this paper was to summarize current video and image defogging algorithms. We first presented a review of the detection and classification method of a foggy image. Then, we summarized existing image defogging algorithms, including image restoration algorithms, image contrast enhancement algorithms, and fusion-based defogging algorithms. We also presented current video defogging algorithms. We summarized objective image quality assessment methods that have been widely used for the comparison of different defogging algorithms, followed by an experimental comparison of various classical image defogging algorithms. Finally, we presented the problems of video and image defogging which need to be further studied. The code of all algorithms will be available at http://www.yongxu.org/lunwen.html.

INDEX TERMS Foggy image classification, image defogging, video defogging, image quality assessment.

I. INTRODUCTION

Fog and haze are a common phenomenon on land and ocean. In foggy and hazy weather, there are many atmospheric particles of significant size. They not only absorb and scatter the reflected light of the scene, but also scatter some atmospheric light to the camera. Thus, the image acquired by the camera is degraded and usually has low contrast and poor visibility [1]. This will seriously influence the visual system especially the visible light visual system. Due to the degradation of the image, the targets and obstacles of the image are difficult to detect. This is bad for automated video processing, such as feature extraction, target tracking, and recognition of objects. This is also one of the main reasons for accidents in the air, on the sea, and on the road. So it is important to design an image defogging algorithm to improve the environmental adaptability of the visual system.

With the development of computer technology, the video and image defogging algorithms have received much attention and are widely applied in civil and military fields, such as remote sensing, target detection, and traffic surveillance. Hautière *et al.* [2] used the image defogging algorithm to enhance the visibility of the vehicle visual system, which can effectively prevent car accidents. For images of outdoor scenes, Narasimhan et al. analyzed the visual manifestations of different weather conditions, such as haze, fog, cloud, and rain [3], and then established an physical imaging model based on the atmospheric scattering phenomenon for image defogging [4], [5]. Because the existing defogging or dehazing algorithms have no clear boundaries, in this paper we use image defogging to refer to algorithms that have the ability to remove fog or haze from the image. Many improved defogging algorithms based on the physical model were proposed for outdoor scenes. Some video and image defogging algorithms were also proposed for real-world traffic surveillance scenes [6]–[9]. In order to improve the visibility of the unmanned surface vehicle (USV) visual system, Ma et al. presented an improved image defogging algorithm based on the dark channel prior to foggy sea image restoration, and the proposed single image defogging algorithm was also extended to fast video defogging [10]. Under poor visibility conditions

such as foggy weather, it is difficult to find runways and hazards from the visual system of a flight. In order to solve this problem, Rajput et al. presented a contrast enhancement algorithm based on the Retinex theory which can effectively improve the visibility of the foggy image acquired by the flight visual system [11]. Most existing defogging algorithms also aim at removing fog from land images. However, there are few studies of the sea and air. The above applications all demonstrate that the video and image defogging algorithms are significant and well worth studying.

In past years, some institutions have done research on image defogging and obtained good results. In America, the Langley Research Center (LRC) of National Aeronautics and Space Administration (NASA) has studied the image enhancement and defogging algorithm since 1995, and their research has made a great contribution to the field of image enhancement based on the Retinex theory.[1] Their algorithms can greatly enhance the visibility of an image acquired under bad weather conditions, such as smoke, haze, underwater, night, or low illumination conditions [11]–[15]. On the DSP microprocessor, their algorithms can reach a speed of 30 frames per second with an image size of 256×256 [16]. The French Central Laboratory of Roads and Bridges made significant progress in enhancing the visibility of the vehicle visual system in foggy weather [2], [17]–[19]. They also established three Foggy Road Image Databases (FRIDA) for benchmarking visibility restoration algorithms.[2] The Computer Vision Laboratory of Columbia University established a weather and illumination database (WILD) which was acquired under a variety of weather and illumination conditions of the outdoor urban scene[3] [3]. They proposed many image defogging algorithms to improve visibility by using multiple images of the same scene [3]–[5], [20]–[23]. A group in the Hybrid Imaging Laboratory of Technion of Israel developed an image defogging algorithm via multiple polarization images[4] [24]–[28]. The Visual Computing Group of Microsoft Research Asia in cooperation with the Chinese University of Hong Kong made significant progress in single image defogging and proposed the dark channel prior to image restoration which obtained vivid restoration effects of outdoor foggy images [29], [30].

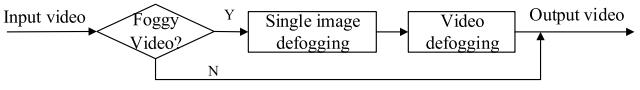

FIGURE 1. A complete video defogging system.

This paper aims to study the image and video defogging algorithms proposed during the last decade. A complete video defogging system is shown in Fig.1. Most of existing video and image defogging algorithms do not take into account the factor of whether there is fog or not. However, for an intelligent defogging algorithm, the judgment method of the foggy and non-foggy image is very important. Thus, in this paper, we will also give a brief summary of it. The structure of this paper is as follows. In Section II, we shall first provide some methods to judge whether an image needs to be processed. Section III summarizes many defogging algorithms for single image defogging. Section IV briefly introduces some recent video defogging algorithms. Section V introduces some quality assessment criteria which are widely used to compare different image defogging algorithms. Experiments are shown in Section VI. Finally, we summarize the paper and present some problems which need to be studied in the future.

II. DETECTION AND CLASSIFICATION OF FOGGY IMAGES

Existing video and image defogging algorithms are always directly applied to the image regardless of the presence or absence of fog. But for real-world applications, it is necessary to know whether the image acquired in the current environment needs to be processed by a defogging algorithm. The main reason is as follows: visibility of the restored image obtained by the defogging algorithm may be worse than the original image if no judgment is made. Also, the use of the defogging algorithm is time consuming, which is not beneficial to realize the real-time target detection, tracking, and recognition. There are two methods which can judge whether the current scene has fog or not. The first method is the fog detection method which regards the invisible area of the image as the foggy area. The second method is the foggy image classification method.

A. DETECTION OF FOGGY AREAS IN IMAGES

Two methods are able to detect the foggy areas of the image. The first method is based on the semi-inverse image, and the second method is based on the meteorological visibility distance.

1) FOGGY AREA DETECTION BASED ON THE SEMI-INVERSE IMAGE

Ancuti et al. first proposed a foggy area detection algorithm based on the 'semi-inverse' image[5] [31]. The semi-inverse image S is obtained by selecting the maximum of the original image pixel and its inverse image pixel which is formulated as

$$S^c(x) = \max[I^c(x), 1 - I^c(x)] \tag{1}$$

where c denotes one of the RGB channels, I is the original image, and $1 - I^c(x)$ denotes the inverse image of the original image.

After renormalizing the inverse image, Ancuti et al. detected the foggy areas in the h^* channel of the Lch color space, and regarded the pixels which have a large difference between the semi-inverse image and original image as clear

[1]More results about the Retinex algorithm are available at: http://dragon.larc.nasa.gov/retinex/background/retpubs.html

[2]FRIDA is available at: http://perso.lcpc.fr/tarel.jean-philippe/index.html

[3]WILD is available at: http://www.cs.columbia.edu/CAVE/software/wild/index.php

[4]More results of the polarization-based defogging algorithm are available at: http://webee.technion.ac.il/~yoav/research/instant-defogging.html

[5]More results of the 'semi-inverse' defogging algorithm are available at: http://research.edm.uhasselt.be/~oancuti/Dehaze_ACCV_2010/

pixels, and regarded the remaining pixels as foggy pixels. This foggy area detection method is based on the fact that the intensity values of pixels in the foggy area of the image are usually much bigger than those of pixels in the clear area. In the sky or foggy areas of an image, pixels usually have a high intensity in all color channels, i.e. $I^c_{fog}(x) > 0.5$. Thus, the semi-inverse image will have the same value as the original image in these areas. However, in clear areas, there is at least one channel of the semi-inverse image where pixel values will be replaced by the inverse image. In other words, the output of Eq.(1) is respectively the original image in foggy areas and the inverse image in clear areas. Then the foggy area can be easily detected by the difference between the original image and its semi-inverse image. This algorithm is simple and effective for detection of foggy areas in foggy images, but it is not suitable for the judgment of whether the current scene has fog or not. This is because the sky area or white area of a clear image will be mistaken for a foggy area via this algorithm.

2) FOGGY AREA DETECTION BASED ON THE METEOROLOGICAL VISIBILITY DISTANCE

The International Commission on Illumination (CIE) defined the meteorological visibility distance of an image and its measurement method [32]. The meteorological visibility distance of an image is widely applied in the field of foggy image detection of a vehicle visual system [33]. For a foggy image, Hautiere and Tarel et al. proposed a daytime foggy area detection algorithm via calculating the meteorological visibility distance [34]. They first used the Canny-Deriche filter to extract the image contours so as to highlight the edges of roadways. Then the region growing algorithm was performed to find the road surface layer. Third, they established four conditions to obtain the target region. Finally, the visibility distance of the image was obtained by calculating the measurement bandwidth. Hautiere and Tarel et al. used a horizontal line to denote the visibility distance. For the vehicle camera system, the region above the horizontal line usually has low contrast and can be regarded as the foggy area or invisible area. Bronte et al. also detected the foggy area of an image via estimating the visibility distance [35].

The fog detection method based on the meteorological visibility distance divides the foggy image into two regions: visible area and invisible area. Although the fog detection algorithm has the ability to detect the foggy area of images, it also has some shortcomings. The invisible area above the horizontal line of the image does not means that it should be absolutely assigned to the foggy area. Some distant scenes of natural clear images also look blurry and may be mistaken for invisible areas or foggy areas by the fog detection algorithm. Moreover, for some foggy images with inhomogeneous fog distribution, it is hard to find a horizontal line to separate the foggy area and clear area. But the meteorological visibility distance can be used to judge which area has thin fog or dense fog. This may be helpful to estimate the parameters of defogging algorithms.

B. CLASSIFICATION ALGORITHM OF FOGGY IMAGES

The foggy image classification method needs to establish an image library which contains large amounts of clear images and foggy images. The method extracts some features which have large difference between the two types of images, and then uses an effective classifier to train the features and obtain the classification hyperplane. Finally, a query image can be classified as a foggy image or clear image. The flowchart of foggy image classification is shown in Fig.2.

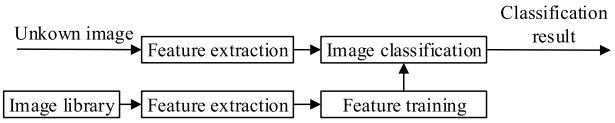

FIGURE 2. The flowchart of foggy image classification.

In the fog classification method, the features are the most important and directly determine the classification accuracy. There is no feature that can accurately classify the foggy image and clear image. Li et al. pointed out that for image visibility, the intensity of the dark channel and image contrast can be used as the feature for the classification of foggy and clear images [36]. Yu et al. extracted the image visibility, the image visual contrast, and the intensity of the dark channel image as features and used the support vector machine (SVM) for foggy image classification [37]. The image visibility is also calculated by the meteorological visibility distance. The measurement of the image visual contrast was first proposed by Jobson *et al.* [38]. Exploiting the atmospheric scattering model, Zhang et al. took the angular deviation between each foggy image and a clear image of the same scene as features for foggy image classification [39]. They also used the SVM to classify the foggy image. Although their method can obtain good classification performance, it is hard to simultaneously obtain a clear image and foggy image of the same scene in real-world applications. Pavlic et al. presented a foggy image classification method by using the global features, in terms of the power spectrum of the Fourier transform and the SVM for the vehicle visual system on highways [40].

Some issues still need to be solved for foggy image classification in the future and the main issues are as follows:

(1) There is no a perfect criterion to judge whether an image is a foggy image or clear image. For example, on sunny days, some distant scenes of natural clear images look blurry. It is hard to determine whether they need to be processed or not. In other words, some images are hard to be assigned to the category of a foggy image or clear image.

(2) It is necessary to find more effective features to recognize foggy images. Because the computational efficiency is important, the features need to be fast extracted. Maybe some quality assessment indexes can be used as features of foggy image classification.

(3) It is significant to judge the fog level of the scene. For some defogging algorithms, if we can get the fog level

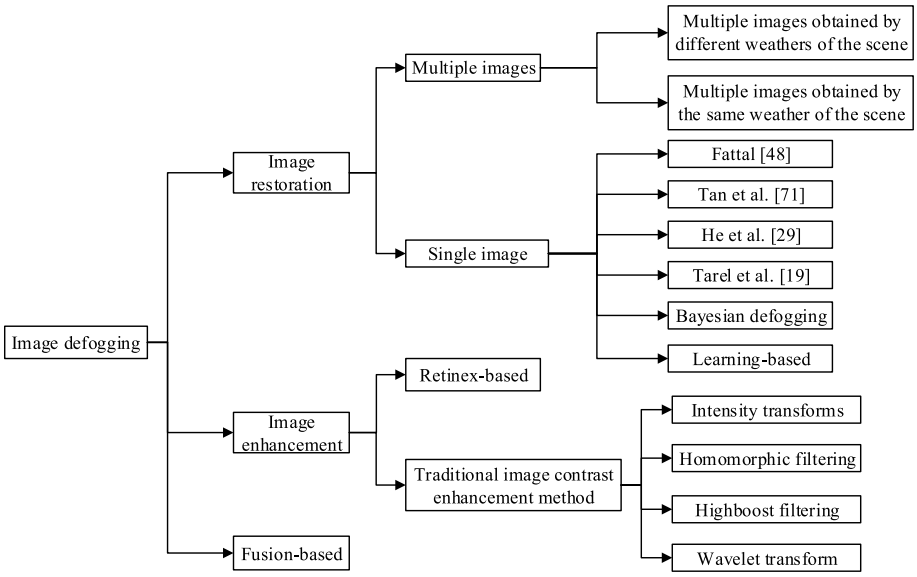

FIGURE 3. The categories of image defogging algorithms.

of the current environment from the image classification, then some parameters of defogging algorithms can be adaptively adjusted to obtain better performance. This is beneficial to video and image defogging in real-world applications. In addition, we can adaptively select the best defogging algorithm in terms of the fog level of the foggy image.

III. IMAGE DEFOGGING ALGORITHM

In some literatures, the image defogging algorithm is simply divided into two categories in terms of whether a physical model is used or not [36], [41]–[45]. The first category is image restoration based on the physical model [19], [22], [46]–[48], and the other is based on image enhancement [49]–[54]. The image restoration method establishes a physical imaging model based on the degradation reason of images under foggy conditions. This category of algorithms needs to estimate the parameters of the physical model, such as the atmospheric light and transmission (depth). The restored image can be obtained by inversely solving the physical model. Image restoration algorithms aim to obtain a natural and clear image which has good visibility while maintaining good performance on color restoration. The second category of defogging algorithms is based on image enhancement and does not take into account the physical imaging model of foggy conditions. It tries to use various image enhancement methods to enhance the contrast and visibility of the foggy image. In recent years, fusion-based defogging algorithms which enhance the image by fusing multiple input images have received much attention [55]–[58]. Thus, fusion-based defogging algorithms can be regarded as the third category of defogging algorithms. The categories of image defogging algorithms are shown in Fig.3.

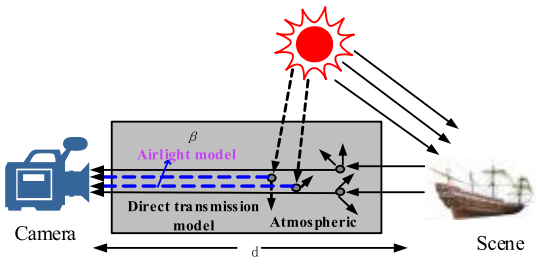

FIGURE 4. Physical atmospheric scattering under foggy conditions [22].

A. IMAGE DEFOGGING BASED ON IMAGE RESTORATION

In 1976, McCartney first proposed the atmospheric scattering physical model based on the Mie scattering theory [59]. Fig.4 shows the physical atmospheric scattering model under foggy weather. The physical model is composed of the airlight model and direct transmission model. Fig.4 also shows the degradation reason of images under foggy conditions. In the direct transmission model, the light for imaging will be attenuated by atmospheric scattering, which leads to the degradation of edge details and object textures of the image. In the airlight model, some sunlight will also be scattered by the atmosphere and transmitted to the camera, and these lights are not the scene lights and can be considered as the fog component of the image whose influence is similar to that of a veil to hide the objects in the image. For a clear image, the direct transmission model makes up a large proportion in the imaging model. With an increase of the concentration of the fog, the proportion of the direct transmission model will decrease while the proportion of the airlight model will increase and visibility of the image will decrease. In other words, the airlight model is the main reason that leads to an image acquired under foggy conditions being a fuzzy image with low contrast and visibility.

Narasimhan and Nayar [5], [23] and Nayar and Narasimhan [60] regarded that the scattering coefficient is not relevant to the wavelength of visible light in the homogenous atmosphere and presented a simplified physical model for image restoration:

$$I(x) = I_\infty \rho(x) e^{-\beta d(x)} + I_\infty (1 - e^{-\beta d(x)}), \tag{2}$$

where I_∞ is the brightness of the sky, $\rho(x)$ is the normalized radiance of a scene point x, β denotes the scattering coefficient of the atmosphere, and $d(x)$ represents the distance between scene point x and the camera. In the right side of Eq.(2), the first item represents the direct transmission model and the second item indicates the airlight model. Eq.(2) also indicates that the proportion of the direct model will decrease due to an increase of the distance. It is also the reason why some distant scenes of the image look blurry on a clear day.

He *et al.* [29] further simplified Eq.(2) as

$$I(x) = J(x)t(x) + A_\infty(1 - t(x)), \tag{3}$$

where J denotes the clear image, t is the transmission, and A_∞ is the atmospheric light value corresponding to an object at an infinite distance and is usually simply estimated from the sky area.

There are only two unknown parameters in Eq.(3). If we can obtain transmission t and atmospheric light value A_∞, then restored image J will be obtained. For the defogging algorithm based on the physical model, the parameters directly determine the defogging result. This means that the more accurately the parameters are estimated, the better the defogging performance will be. We should point out that the simplified physical model is based on the assumption of single-scattering and homogeneous atmospheric medium, so this model may be not the best imaging model for some cases, such as sea fog or inhomogeneous fog.

In the past years, many image restoration algorithms based on the physical model have been proposed and can be divided into two categories based on the number of the image used: the first is image restoration based on multiple images and the second is image restoration based on a single image [61], [62].

1) IMAGE RESTORATION BASED ON MULTIPLE FOGGY IMAGES

Image restoration algorithms based on multiple images can be divided into two categories as shown in Fig.3. The first uses multiple foggy images obtained under the same weather of the scene. The second uses multiple images of the scene acquired under different weather conditions.

a: MULTIPLE IMAGES OBTAINED UNDER THE SAME WEATHER OF THE SCENE

Because the fact that the airlight scattered by atmospheric particles is partially polarized, references [24], [26]–[28], [63] proposed some novel image defogging algorithms by using multiple polarization images. Treibitz et al. compared the image restoration effect with either one or two polarization images, and demostrated that using two polaization images reduces the noise for image restoration [64]. The polarization images with different brightnesses of the same circumstance of the scene are obtained by using a polarization filter with different orientations. This type of image restoration algorithms uses at least two polarization images to estimate the parameters of the physical model and then inversely solves the physical model for image restoration.

Schechner et al. first discussed an image restoration algorithm by using two polarization images [28]. The two polarization images are captured through parallel and perpendicular orientations, respectively. The image defogging algorithms based on polarization images assume that the direct transmission is unaffected by the orientation, and the two polarization images are respectively defined as Eq.(4) and Eq.(5).

$$I^\perp = \frac{D(x)}{2} + V^\perp(x), \tag{4}$$

$$I^\parallel = \frac{D(x)}{2} + V^\parallel(x), \tag{5}$$

$D(x) = J(x)t(x)$ is the direct transmission model. $V^\perp$ and $V^\parallel$ are the airlight model of the parallel and perpendicular polarization images, respectively.

$$V^\perp(x) = A_\infty^\perp(1 - t(x)), \tag{6}$$

$$V^\parallel(x) = A_\infty^\parallel(1 - t(x)), \tag{7}$$

where $A_\infty^\perp$ and $A_\infty^\parallel$ are the atmospheric light values of the two parallel and perpendicular polarization images and can be estimated from the sky area. The degree of polarization is

$$p \equiv \frac{V^\perp - V^\parallel}{V^\perp + V^\parallel}. \tag{8}$$

In the polarized defogging method, the degree of polarization p and atmospheric light A_∞ of each polarization images are the key parameters for estimating restored image J.The degree of polarization can be estimated by two atmospheric light values of the polarization images as

$$\widehat{p} = \frac{A_\infty^\perp - A_\infty^\parallel}{A_\infty^\perp + A_\infty^\parallel}. \tag{9}$$

Then the airlight model and transmission can be estimated from Eq.(4)-Eq.(9).

$$\widehat{V}(x) = \frac{V^\perp(x) - V^\parallel(x)}{\widehat{p}}, \tag{10}$$

$$t(x) = 1 - \frac{\widehat{V}(x)}{A_\infty^\perp + A_\infty^\parallel}. \tag{11}$$

Thus, the restored image can be achieved by using transmission t and airlight model $\widehat{V}(x)$ to inversely solve the physical model of Eq.(3). The original image defogging algorithm based on polarization images does not take into account the problem that the natural image acquired on a

clear day also encounters airlights scattering. So it is possible to get a more natural restored image by preserving part of airlights. Motivated by this idea, Schechner et al. proposed an improved algorithm by multiplying a coefficient to the polarization degree i.e. $\widehat{p} = \varepsilon p$ $(1 \leq \varepsilon \leq 1/p)$ [26]. Miyazaki et al. estimated the parameters by using two traffic signs of the traffic image as the reference [63]. Their algorithm needs to set up a traffic sign database for finding the two traffic signs, which is hard to satisfy the need of real-time processing. Considering that some images do not have a sky area, Shwartz *et al.* [27] proposed a novel method to estimate A_∞ by selecting two similar features in the scene. In order to inhibit noise amplification of the polarization-based dehazing algorithm, an adaptive regularization approach was proposed to further optimize the restored image [64].

In the polarization-based defogging algorithm, the value of A_∞ is manually estimated. Although the polarization-based defogging algorithm has better performance than some algorithms based on optical filtering, the manual operation is not helpful to automatically remove the haze. The polarization-based defogging algorithm is based on the partial polarization of airlight. Therefore, its effect will decrease as the polarization degree decreases. Moreover, it will fail in dense foggy weather. Also, for some scenarios especially the scenario with a moving camera, it is hard to acquire two polarization images since the scenes change more rapidly than the filter rotation.

b: MULTIPLE IMAGES OBTAINED UNDER DIFFERENT WEATHER CONDITIONS OF THE SCENE

Narasimhan et al. studied the image restoration algorithm by using two or more images which were acquired under different weather conditions [3]–[5], [21]–[23]. Narasimhan et al. analyzed the visual manifestations of different weather conditions, and then presented a physical dichromatic atmospheric scattering model [60]. Based on this model, they presented a geometric framework for scene understanding under foggy weather and computed the three-dimensional structure and color of the scene from two or more foggy images [21]. But if the color of the object in the scene is similar to that of fog or haze, it is instable for defogging using this model. In order to solve this problem, a monochrome atmospheric scattering model was presented [22]. Narasimhan et al. also presented a fast image defogging algorithm based on this model [22]. First, the depth discontinuities and the scene structure can be computed by the changes of intensities of the two images of the scene under different weather conditions. Then the contrast can be enhanced via using the scene structure. They also extended their algorithm to video defogging, which was able to enhance the visibility of the surveillance scene.

Above image restoration algorithms are only suitable for surveillance scenes. For other dynamic scenes especially for vehicle cameras, these algorithms will fail because the above two images are hard to be simultaneously acquired. We should point out that the monochrome atmospheric scattering model only describes how scene intensities are affected by homogeneous weather conditions, so it will fail in weather with inhomogeneous fog or haze.

2) IMAGE RESTORATION BASED ON A SINGLE FOGGY IMAGE

Compared to image restoration algorithms using multiple images, single image restoration algorithms have many advantages and have received much attention in recent years [19], [29], [47], [65]–[68]. Single image defogging algorithms are able to enhance arbitrary foggy images under any condition.

As discussed in previous sections, transmission t and atmospheric light value A_∞ are the key parameters for inversely solving the physical model. But the physical model of Eq.(3) is an underdetermined equation, so we should use some prior knowledge to estimate the above two parameters.

a: RESTORATION ALGORITHM OF FATTAL

Fattal presented a method to estimate the transmission and atmospheric light based on the assumption that surface shading and transmission are locally uncorrelated[6] [48]. He presented a refined physical model via two decomposition steps. He first decomposed unknown clear image J to the product of surface albedo coefficients R and shading factor l i.e. $J = Rl$. Then he further decomposed R into two components. One component was parallel to the atmospheric light A_∞ and the other was a residual component R'. The independent component analysis (ICA) algorithm [69] and a Gauss-Markov random field model [70] were used to calculate transmission t. Atmospheric light A_∞ was estimated by using the ICA algorithm based on the assumption that surface shading and transmission are uncorrelated in a small window. The defogging method of Fattal uses the statistical property to estimate parameters for image restoration. Thus, the performance greatly depends on the input image. The method will fail when the image has dense fog and insufficient signal-to noise ratio.

b: RESTORATION ALGORITHM OF Tan et al.

Tan et al. proposed an automated defogging algorithm based on a single image according to two basic observations: first, the clear or enhanced images usually have higher contrast than foggy images and second, the airlight changes smoothly in a small local area [71]. Tan et al. first used the white balance operation to transform the input image into white color. Then the Markov random field was used to model the airlight model. Based on this model, the airlight could be estimated via maximizing the local contrast of the restored image. Their algorithm can automatically enhance the visibility of a foggy image and does not need any user interaction. In their proposed method, the global parameter of atmospheric light A_∞ is simply estimated by the highest

[6]The code of Fattal's algorithm is available at: http://www.cs.huji.ac.il/~raananf/projects/defog/

intensity of the input image. The purpose of their method is to obtain a restored image which has maximum contrast. They do not take into account color restoration, which gives color distortion to the enhanced image. Because the patch-based operation is used to estimate the airlight model, some 'halo' effect may also appear in the resulting image especially in depth discontinuities areas.

c: RESTORATION ALGORITHM OF He et al. AND THEIR IMPROVED ALGORITHM

In order to solve the above problems, He et al. proposed a novel defogging algorithm based on a single image, which has proved to be an effective method to restore outdoor images[7] [29].

He et al. studied a large amount of clear outdoor images and found that in most areas of a clear outdoor image (except for the sky area and white area), there is a channel of pixels with the minimum value of zero. This is also called the dark channel prior theory. The dark channel image is calculated by

$$J^{dark}(x) = \min_{c\in\{r,g,b\}} (\min_{y\in\Omega(x)} (J^c(y))), \tag{12}$$

where Ω denotes a square window centered at pixel x, and r, g, and b are the red, green, and blue components, respectively. For a clear image except for the sky area and white area, $J^{dark} \approx 0$.

According to their findings, He *et al.* [29] first proposed a dark channel prior (DCP) theory to estimate the transmission for image restoration by taking the following min operation in the local area on Eq.(3)

$$\min_{c\in\{r,g,b\}} (\min_{y\in\Omega(x)} (\frac{I^c(y)}{A^c_\infty})) = t(x) \min_{c\in\{r,g,b\}} (\min_{y\in\Omega(x)} (\frac{J^c(y)}{A^c_\infty})) + (1 - t(x)). \tag{13}$$

In terms of Eq.(12) and Eq.(13), coarse transmission $\tilde{t}$ is

$$\tilde{t}(x) = 1 - \min_{c\in\{r,g,b\}} (\min_{y\in\Omega(x)} (\frac{I^c(y)}{A^c_\infty})). \tag{14}$$

Because of the use of the min filtering in the local area of the dark channel image, the dark channel image will have block artifacts (halo artifacts). This will also cause the restored image to have block artifacts. In order to solve the block artifacts, the original DCP defogging algorithm used a soft matting operation to optimize the transmission. In the original DCP algorithm, atmospheric light value A_∞ was also obtained via the DCP theory. He et al. first selected a local area in the dark channel image which had the top 0.1% brightest pixels, and then simply chose the pixel with the highest intensity of the original foggy image in the selected area as atmospheric light A_∞. Finally, restored image J was obtained using

$$J = \frac{I(x) - A_\infty}{\max(t(x), t_0)} + A_\infty, \tag{15}$$

where t denotes the optimized transmission via soft matting and t_0 is a small constant used to prevent the zero denominator.

The DCP defogging algorithm can effectively remove the fog from an outdoor foggy image. Gibson et al. provided a mathematical explanation why the DCP theory works well for image defogging [72]. The more various color information the foggy image has, the better the restoration effect will be. But if the image has a large sky area, large white area, or dense fog and inhomogeneous fog, the DCP theory will fail. Moreover, the soft matting algorithm to refine the transmission is time consuming and cannot be applied in practical applications. Nevertheless, if we use the coarse transmission for image defogging, the resulting image will have halo artifacts caused by the patch-based min filtering. Huang et al. analyzed the drawback of the original DCP defogging algorithm and proposed an improved DCP algorithm with three modules for single image defogging [47]. Their algorithm can also enhance sandstorm images. In order to improve the efficiency, Xie et al. proposed to use the multiscale Retinex algorithm to estimate the transmission [73]. Gibson et al. also used median filtering to optimize the transmission [46], [74]. In addition, their work demonstrated that performing the defogging algorithm before image compressing is better than defogging after compressing [74]. But using median filtering may cause edge degradation. Some researchers tried to use filters which have good performance in preserving edge information to replace the soft matting algorithm. For example, the weighted least square (WLS) based edge-preserving smoothing method [75], locally adaptive Wiener filter [76], bilateral filtering [77], and joint bilateral filtering [78] are good candidates. He et al. proposed a guided image filtering[8] method which proved to have a better edge preservation effect and was faster than bilateral filtering and joint bilateral filtering [30]. Then some improved defogging algorithms were further proposed based on guided image filtering. For example, Pei et al. used the DCP theory and guided image filtering to restore the night-time haze image [79]. Chen proposed an improved DCP defogging algorithm by using a pair of visible light (VL) and near-infrared (NIR) images to restore the near-infrared image [80]. In order to improve the defogging efficiency, Lin and Wang [9] first resized the transmission by using the down-sampling algorithm, and then used guided image filtering to optimize the transmission. Using the edge-preserving filters above to replace the soft matting algorithm for image defogging not only can greatly improve the efficiency, but also obtains a better edge restoration effect.

Meng et al. proposed an improved DCP defogging algorithm by imposing an inherent boundary constraint on the transmission function and using the weighted L_1-norm based contextual regularization to optimize the transmission[9] [81]. In this algorithm, the restored image is always bounded

[7]More results and information of the DCP defogging algorithm are available at: http://research.microsoft.com/en-us/um/people/kahe/cvpr09/index.html

[8]More information about the guided image filtering are available at: http://research.microsoft.com/en-us/um/people/kahe/eccv10/

[9]More results and code of Meng's DCP defogging algorithm are available at: http://www.escience.cn/people/menggaofeng/research.html

as $C_0 \le J(x) \le C_1$, and the coarse transmission map is

$$\tilde{t}(x) = \max_{y\in\omega(x)} \left\{ \min \left[\max_{c\in\{r,g,b\}} \left(\frac{A^c - I^c(y)}{A^c - C_0^c}, \frac{A^c - I^c(y)}{A^c - C_1^c} \right), 1 \right] \right\}, \tag{16}$$

where C_0 and C_1 are the two boundary constraints of the transmission map and A is the atmospheric light which is selected as the highest intensity of each channel after performing minimum filtering and maximum filtering with a moving window.

Meng *et al.* [81] used the following optimal transmission function with the weighted L_1-norm based contextual regularization for optimizing the coarse transmission map

$$\frac{\lambda}{2} \left\| t - \tilde{t} \right\|_2^2 + \sum_{j\in\omega} \left\| W_j \circ (D_j \otimes t) \right\|_1, \tag{17}$$

where λ is the regularization parameter for balancing the two terms of the objective function, W is a weighting matrix, D is a first-order differential operator, and $\circ$ and $\otimes$ are the element-wise multiplication operator and convolution operator, respectively. Fine transmission t can be obtained by minimizing the above objective function. This transmission optimization algorithm has good effect on the restoration of foggy images, but fine transmission is obtained by iteration computation which is time consuming. The number of iterations and the two boundary constraints cannot adaptively adjust.

d: RESTORATION ALGORITHM OF Tarel et al.

As the soft matting algorithm is too complex, Tarel et al. proposed a fast image restoration algorithm by using median filtering and its variant to replace the soft matting algorithm[10] [19]. The algorithm of Tarel et al. can real-time process color or gray images. In this algorithm, the atmospheric light value A_∞ is set to (1, 1, 1) via the white balance algorithm. Because min filtering is the reason of the block effect in the restored image, they only used the dark channel image to estimate the atmospheric veil. For each pixel, they assumed that the atmospheric veil $V(x)$ was less than the minimal component of the original foggy image. They wanted to obtain the maximum V which is smooth in most areas except for the edge area of the image. In order to improve the efficiency while preserving the edge and corner, they exploited the median filtering and its variant. First two median filtering operators were used to acquire the following coarse atmospheric scattering veil

$$V(x) = \max(\min(pB(x), W(x)), 0), \tag{18}$$

$W(x) = \min_{c\in\{r,g,b\}} (I^c(x))$ is the minimal component of the original foggy image, $B(x) = C(x) - \underset{y\in\Omega(x)}{median}(|W - C|(y))$, $C(x) = \underset{y\in\Omega(x)}{median}(W(y))$, $p \le 1$ and p denotes the restoration degree, p is usually set to a constant in the range of [0.9,0.95], and Ω is the diameter of the median filtering window.

Tarel et al. proposed a Median of Median Along Lines algorithm to achieve the optimal coarse atmospheric scattering veil. The restored image then can also be obtained by Eq.(3). The defogging algorithm of Tarel et al. can restore both gray and color images.

e: Bayesian DEFOGGING

Based on the fact that the scene albedo ρ and depth d are two statistically independent components, Kratz and Nishino proposed a Bayesian defogging algorithm for single image defogging[11] [65], [82]. They first factorized the image into the scene albedo and depth as

$$\ln(1 - \frac{I(x)}{I_\infty}) = \ln(\rho(x) - 1) - \beta d(x). \tag{19}$$

They defined $\tilde{I}(x) = \ln(1 - \frac{I(x)}{I_\infty})$, $C(x) = \ln(\rho(x) - 1)$, and $D(x) = -\beta d(x)$. $C(x)$ and $D(x)$ can be viewed as the items of the scene albedo and depth, respectively. Then a Factorial Markov Random Field (FMRF) was applied to model the dependence between these two items and the input image

$$p(C, D|\tilde{I}) \propto p(\tilde{I}|C, D)p(C)p(D). \tag{20}$$

Scene albedo C and depth D were estimated via maximizing Eq.(20). The restored image was then achieved by inversely solving the physical model.

Wang et al. presented another depth map estimation algorithm via multiscale depth fusion based on Bayesian theory and Markov regularization[12] [53]. They first assumed that each prior depth map p_i was composed of noise ε_i and true depth maps t as follows

$$p_i(x) = H_i(x)t(x) + \varepsilon_i(x), \quad i = 1, \ldots, m, \tag{21}$$

where H_i is the weight which denotes the contribution degree of the true depth map to the prior map. They used the Gaussian function to model the noise. Then the true depth map was estimated by maximizing the following posteriori function

$$t = \arg\max \{P(D|p_1, \ldots, p_m)\}. \tag{22}$$

They used the Gibbs distribution to model $P(D)$ and transformed Eq.(22) to an energy function defined as

$$t = \arg\max_t \{E(t)\}, \tag{23}$$

where $E(t) = U(t) + \sum_i \sigma^{-2}(p_i - t)^T(p_i - t)$. The first term $U(t)$ is the smoothing term with both smoothing and edge-preservation constraints, and the second term can be viewed as the noise component. After the iteration computation of the energy function, the fine depth map and restored image can be achieved. The algorithm is effective in reducing the

[10]The code and image set of Tarel's defogging algorithm are available at: http://perso.lcpc.fr/tarel.jean-philippe/publis/iccv09.html

[11]More results of Bayesian defogging are available at: https://www.cs.drexel.edu/~kon/defog/index.html

[12]More results of Wang's algorithm are available at: http://www.ykwang.tw/single-image-defogging.html

halo artifacts, but the iteration is time consuming, and the parameters need to be set manually.

f: LEARNING-BASED RESTORATION ALGORITHM

Tang et al. proposed a novel transmission estimation method via a learning-based approach [83]. They used the Random Forest to learn a regression model which revealed the relation between the haze-relevant features and their true transmission of image patches. For an unknown foggy image, the image is first divided into several small patches and haze-relevant features are extracted, and then the learned Random Forest model is used to obtain the transmission of each image patch. After that, the coarse transmission is obtained by aggregating the transmission of each image patch. The algorithm also uses the guided image filtering to further optimize the transmission. The learning-based algorithm has the ability to learn adaptive regression models for different weather conditions, which is able to restore the foggy image with inhomogeneous fog or dense fog. But the learning-based algorithm also has many shortcomings. The algorithm needs many fog-free and foggy image pairs as training data for learning the regression model, but it is hard to obtain a large number of training data. The coarse transmission which is estimated by the regression model is not the true transmission of the image. It cannot reveal the true depth information of the image especially edge areas.

B. IMAGE DEFOGGING BASED ON IMAGE CONTRAST ENHANCEMENT

Image contrast enhancement algorithms aim to improve the contrast of the image and are widely used in the field of image defogging, underwater image enhancement, and medical image enhancement.

1) IMAGE DEFOGGING BASED ON THE RETINEX THEORY

Edwin Land first proposed the Retinex theory based on color constancy [84]. The term Retinex comes from two words ''retina'' and ''cortex'', which indicates biological visual perception. The Retinex theory has been widely applied in the field of image defogging, dark image enhancement, and Mars Express image enhancement [12], [85]–[87].

The Retinex theory considers that an image is composed of the incident component and reflection component. The incident component represents the luminance information of an image, and it is also called the luminance image. The reflection component expresses the inner information of an image, and it is also called the reflection image. The Retinex model is shown in Fig.5.

Based on the the Retinex theory, the image $S(x, y)$ can be described as

$$S(x, y) = L(x, y) \cdot R(x, y), \tag{24}$$

where $S$is the original foggy image, R is the reflection component, L is the incident component, and (x, y) are the position coordinates of the image.

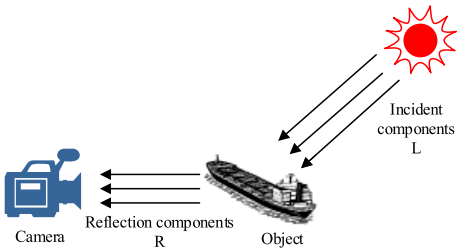

FIGURE 5. Retinex model [85].

The Retinex-based defogging algorithm achieves the reflection image by solving the Retinex model. In order to obtain R from S, the logarithm is applied to both sides of Eq.(24).

$$\log S(x, y) = \log L(x, y) + \log R(x, y). \tag{25}$$

From Eq.(25), if we can obtain L, then R can be obtained. So the estimation of L directly determines the effect of image defogging. In order to estimate the incident component, the random path-based algorithm [88], the passion equation-based iteration algorithm [89], and the multiple-scale algorithm based on the difference-of-Gaussian (DOG) operator were proposed in early studies. Hurlbert et al. summarized the above estimation methods of the incident component [90]. In addition, McCann et al. proposed two Retinex algorithms based on the multi-resolution pyramid: the McCann99 Retinex algorithm and the Frankle-McCann Retinex algorithm[13] [91], [92]. The goal of the Retinex algorithm for image enhancement is to simultaneously realize the dynamic range compression, color constancy, and color/lightness rendition [93]. The above estimation algorithms are very complex and do not achieve good performance in color constancy. Because the Gaussian function has good performance over a wide range of space constants, Jobson et al. proposed to use the Gaussian function to estimate the incident component [93], [94]. This is also the original single scale Retinex (SSR) algorithm, in which the incident component is estimated by

$$L(x, y) = S(x, y) * G(x, y), \tag{26}$$

where"$*$" represents the convolution operation. Gaussian function $G(x, y)$can be expressed as $G(x, y) = k \cdot \exp\left(-\frac{x^2+y^2}{\sigma^2}\right)$, where σ is the scale parameter of the Gaussian function and k is a normalizing factor which is used to ensure $\iint G(x, y)dxdy = 1$. For a RGB image, the reflection image is achieved:

$$r_i(x, y) = \log(S_i(x, y)) - \log(S_i(x, y) * G(x, y)), \tag{27}$$

where $r(x, y) = \log R(x, y)$, $i \in \{r, g, b\}$ is one of three channels of a RGB image. In the SSR algorithm, the performance of image enhancement is determined by scale

[13]The matlab code of the McCann99 Retinex algorithm and the Frankle-McCann retinex algorithm are available at: http://www.cs.sfu.ca/~colour/code/

parameter σ. If the value of σ is large, then the enhanced image preserves good color/lightness rendition, but the restoration of image details is not good. Otherwise, the opposite effect could be obtained. In other words, the SSR algorithm cannot simultaneously achieve dynamic range compression and color/lightness rendition.

In order to overcome the above drawback, the multiscale Retinex (MSR) algorithm and the multiscale Retinex with color restoration (MSRCR) algorithm were proposed [12], [13], [93], [95], [96]. Different from the SSR algorithm, the MSR algorithm applies three normalized Gaussian filters with different scales in each channel, which can be viewed as the weighted sum of the outputs of three SSR algorithms with different scales and is defined as

$$r_i(x,y) = \sum_{j=1}^{3} \omega_j \left[\log S_i(x,y) - \log(S_i(x,y) * G_j(x,y)\right], \quad (28)$$

where ω_j denotes the weight of each scale. In the MSR algorithm, the three weights are all equal to 1/3. The three scales of Gaussian function are set to 15, 80, and 250 for most images [96]. Finally, a gain/offset algorithm is used to transform the reflection component into the display domain [0, 255].

The MSR algorithm has the advantages of small scale dynamic range compression, image edge detail enhancement. and big scale color balance. But the MSR algorithm cannot achieve good color restoration. To solve this problem, the MSRCR algorithm uses a color restoration step to control the saturation as

$$r_i(x,y) = C_i(x,y) \sum_{j=1}^{3} \omega_j \times \left[\log S_i(x,y) - \log(S_i(x,y) * G_j(x,y)\right], \quad (29)$$

where C_i is the color restoration function. After the reflection component is obtained by Eq.(29), the output also needs to be transformed into the display domain. Moore et al. presented an automatic normalization method to deal with the output of the Retinex-based algorithm [97]. Jobson et al. presented a 'canonical gain/offset' algorithm to transform the output into the display domain [96].

Petro et al. analyzed SSR, MSR, and MSRCR algorithms and pointed out that the color restoration function was at risk of inverting colors, and then presented a color restoration method which was applied to the intensity channel [98]. The source code and the online demo are accessible at a homepage.[14]

The fog is the low-frequency component of the image. In order to enhance an outdoor foggy image scene, Wang et al. first used the wavelet transform to enhance the foggy image, and then used the SSR algorithm to improve the brightness to achieve a fog-free image [49]. Zhao et al. used the nonlinear sigmoid function to replace the logarithm function in the MSR algorithm for foggy image defogging [54]. The original SSR, MSR, and MSRCR algorithms use Gaussian filtering to estimate the incident component, which will lead to edge degradation of the enhanced image. The reason is that Gaussian filtering does not have good edge preservation performance. In order to solve this problem, Hu et al. first used the bilateral filter to estimate the incident component, and then used the Gamma adjustment and sigmoid function to further enhance the reflection image [99]. Yang et al. proposed a novel variable filter Retinex algorithm which adaptively selected the scale parameters for every local area of the foggy image [100]. The proposed algorithm can greatly enhance the local contrast of the image and improve the visibility.

[14]More results of Petro et al. are available at: http://www.ipol.im/pub/art/2014/107/

2) IMAGE DEFOGGING BASED ON THE TRADITIONAL IMAGE CONTRAST ENHANCEMENT METHOD

In this section, we will briefly summarize the image defogging algorithm based on the traditional image contrast enhancement method, such as the intensity transforms, homomorphic filtering, high-boost filtering, and wavelet.

a: INTENSITY TRANSFORMS

The histogram of the foggy image is usually distributed centrally since most pixels have large color values or gray values. Thus, the foggy image has low contrast and dynamic range. Intensity transforms are a simple and effective method which enhances the image by redistributing the histogram [101]. The power-law gamma transformation, piecewise-linear transformation, and histogram equalization (HE) are typical contrast enhancement algorithms and are widely used in the field of night image enhancement, X-ray image enhancement, and image defogging. In the field of image defogging, the power-law gamma transformation and piecewise-linear transformation are usually applied in the last step, which is used to improve the brightness of the enhanced image. Gao et al. [102] applied it to each channel of the enhanced image obtained by the MSR algorithm. In the Retinex-based algorithm, the gain/offset step which is used to transform the reflection component to the display domain can also be regarded as a special piecewise-linear transformation. Ma et al. used the piecewise-linear transformation to further improve the visibility of the enhanced image obtained by the SSR algorithm [85].

The HE method enhances the image by redistributing the image histogram to expand its dynamic range. The HE method is divided into two categories: global histogram equalization (GHE) and local histogram equalization (LHE) [52], [103]. The GHE algorithm can enhance the global contrast of a foggy image, but it cannot enhance the local contrast of a foggy image. For foggy images with an inhomogeneous fog distribution, the GHE algorithm cannot achieve good performance. Especially in the depth discontinuities area, the GHE algorithm leads to halo artifacts. Jun and Rong [104] used the GHE algorithm to first enhance the foggy image, and then used the wavelet transform to reduce halo artifacts and noise.

In order to enhance the local information of an image, various LHE algorithms and their improvements have been proposed [103], [105], [106]. Kim proposed a partially overlapped sub-block histogram equalization (POSHE) algorithm. The POSHE algorithm first performs the GHE algorithm on each sub-block, and then applies a weighted fusion strategy to the overlapped pixels [103]. The POSHE algorithm not only improves the contrast of the image, but also reduces the 'block' artifacts. Patel et al. compared the performance of brightness preservation of many local histogram equalization algorithms [107]. Ramya et al. proposed a brightness preserving dynamic fuzzy histogram equalization (BPDFHE) algorithm to enhance the visibility of foggy images and to maintain color fidelity [7]. In order to reduce the noise caused by the HE algorithm, the contrast limited adaptive histogram equalization (CLAHE) was proposed [108]. Xu *et al.* [8] performed the CLAHE algorithm on the intensity component of the HIS space to enhance the visibility of a foggy image while reducing the noise.

Even though image contrast can be enhanced by histogram stretching, the image often appears unrealistic. This simple technique will fail when the image has significant depth variations or there is inhomogeneous fog or haze. Directly performing the HE algorithm on each channel will change the color structure of foggy images, which causes the HE algorithm to suffer from a color distortion problem. Although we can only apply the HE algorithm to the intensity channel to reduce the color distortion, the enhanced image also encounters the problem of color degradation due to the influence of the intensity on all channels of an image of the fog. However, for some foggy images with dense fog, the visibility of the enhanced image obtained by the HE-based algorithm is better than other methods, such as the Retinex-based algorithms and physical model-based algorithms.

b: HOMOMORPHIC FILTERING

In general, in the frequency domain, the high-frequency components of an image are associated with the image area whose intensity dramatically changes, such as the edge of the image. The low-frequency components represent the flat area of an image including the sky area. The airlight component of the physical model can be regarded as the main component of low-frequency. The edge information of a foggy image is usually degraded owing to the influence of fog. In other words, the high-frequency components are decreased while the low-frequency components are increased. So if we can improve the high-frequency components and weaken the low-frequency components of an image, the visibility of a foggy image may be enhanced. The homomorphic filtering method has a model similar to the Retinex theory, but it does not need to estimate the incident component [109]. Homomorphic filtering enhances an image by using high pass filtering to enhance the high-frequency components and reduce the low-frequency components. This algorithm is simple and fast, but it also cannot enhance a foggy image with dense fog or inhomogeneous fog.

c: HIGH-BOOST FILTERING

High-boost filtering also enhances an image by amplifying the high frequency component [101]. High-boost filtering and Retinex-based algorithms also have some similarities. The mask image of high-boost filtering can be viewed as the reflection image of the Retinex-based algorithm. High-boost filtering fuses the mask image and original image to improve the high frequency component, which can enhance the visibility and edge information of the image. This algorithm is also simple and fast. The visibility can be enhanced by the algorithm, but it will cause color distortion and noise amplification.

d: WAVELET TRANSFORM

Similar to homomorphic filtering and high-boost filtering methods, the wavelet transform also enhances an image by improving the high frequency component and reducing the low frequency component [110]. Busch et al. proposed a fog visibility analysis method via the wavelet transformation for a traffic control system [111]. Jia and Yue [112] first used the wavelet transform to decompose the luminance component of the YUV space, then removed the airlight model by applying Gaussian filtering to the low-frequency sub-bands, and used the high-pass filter to enhance the image information in the high frequency sub-bands. Finally, the enhanced image was obtained via the inverse wavelet transform. Rong et al. used the unsharp masking algorithm to enhance the contrast of the low-frequency [113]. The wavelet-based algorithm has good performance in reducing the halo effect and noise, but the visibility cannot be improved especially for images with heavy fog or inhomogeneous fog. This is mainly because the filter used is simple and does not take into account the information of the scene. In other words, the fog component and edge information cannot be well estimated via the simple filtering. Yang et al. combined the wavelet transformation and physical model for image defogging [114]. They used the low frequency obtained by the wavelet transform to estimate the coarse transmission, and then used the guided image filtering to optimize the transmission for image defogging.

C. IMAGE DEFOGGING BASED ON THE FUSION STRATEGY

Fusion algorithms of the near-infrared and visible light images have been applied in many fields, such as face recognition, target detection, target tracking, and recognition [115]–[117]. In general, the scattering in near-infrared (NIR) is less than that in visible light (VL). So the NIR image has more detailed information and higher contrast than the VL image under foggy weather. Based on this fact, Schaul et al. proposed to fuse the NIR image and VL image to enhance the visibility of a foggy image [58]. Two original images were directly fused via the weighted least squares optimization framework. Their algorithm will fail if the NIR image has very low contrast under the condition of dense foggy weather. The NIR image defogging and VL image defogging will be another research direction in the

TABLE 1. The comparison of some typical image defogging algorithms.

Defogging method	Advantages	Disadvantages	Applications
Multiple images obtained under different weather conditions of the scene	Colors are restored well.	(1) Hard to obtain the source images. (2) Fail to restore dense foggy images or inhomogeneous foggy images.	Special applications such as surveillance and thin foggy weather.
Multiple images obtained under the same weather of the scene	Good color fidelity, high image visibility under thin fog.	(1) Atmospheric light value is manually set. (2) Fail to restore the dense foggy image. (3) Hard to take the source images.	The scene with unmoving camera and thin foggy weather.
Fattal [48]	High image visibility under inhomogeneous fog or thin fog.	Fail to enhance the image with dense fog or insufficient signal-to-noise ratio.	Single color foggy image.
Tan et al. [71]	Good contrast of the foggy image.	Foggy image may be overly restored and accrued 'Halo' effect and color distortion.	Single color or gray foggy image.
He et al. [29,30]	Resultant image is an approximate natural clear image and has good color restoration effect.	(1) Fail to restore image under inhomogeneous fog weather and dense fog weather. (2) Fail to restore the image with large sky area or large white area.	Single color image especially outdoor image with thin fog.
Tarel et al. [19]	(1) Fast. (2)High visibility for thin foggy images.	(1) Color distortion. (2) Fail to process the image with discontinuous scene depth.	Single color or gray image.
Bayesian defogging [53]	Little halo effect and high visibility for foggy images.	(1) High computation cost. (2) May lead to edge degradation and color distortion.	Single color foggy image especially thin foggy image.
Learning-based [84]	Maybe suitable for all scenes.	(1) Hard to obtain the large dataset. (2) The lack of a perfect learning model. (3) The current algorithm is not mature enough.	Color image.
Retinex-based	Simple and fast. Very suitable for the foggy image with low intensity.	(1) Fail to enhance the foggy image with inhomogeneous fog. (2) Cannot enhance the local information of the foggy image.	Single color or gray image. The visibility of the image with low intensity can be improved.
Intensity transforms	Resultant image has high contrast.	(1) Color and edge distortion. (2) Boost noise. (3) 'Halo' effect.	Single color or gray image especially the image with thin fog and same depth.
Wavelet transform	Highlighted local information or edge information of the foggy image. Good noise suppression.	(1) Fail to enhance the image with dense fog or inhomogeneous fog. (2) May make the resultant image too bright or too dark.	Single color or gray image especially the image with thin fog or homogeneous fog.
Fusion-based algorithms	Generally speaking, fusion-based algorithms can obtain better performance than single image defogging algorithms.	Fusion approach is complex and leads to a low efficiency.	Single color or gray image.

future, which will be useful to improve the performance of target detection, tracking, and recognition.

Ancuti et al. proposed a fusion-based single image defogging algorithm via fusion of several images derived from the original foggy image [31]. They first used the semi-inverse approach (see Section A(1)) to detect the foggy area in a foggy image and then estimated the atmospheric value A_∞ in clear areas. Then several images are obtained using

$$L_i = I - a_i \cdot A_\infty, \tag{30}$$

where a_i is a constant value in the range [0, 1]. $i \in [1, k]$, k denotes the number of images used for fusion, and I is the original foggy image. Then the foggy area detection operation is performed on each image L_i and the area with low hue disparity of the corresponding image L_i is selected as the final input image for fusion. Finally, they achieved the restored image via a simple weighted fusion of the input images.

The above algorithm is based on foggy area detection via the semi-inverse image. For some scenes, especially sea scenes, haze detection based on the semi-inverse method will fail due to the little difference between the original image and the inverse image. This means if foggy area detection fails, a bad performance will be obtained.

In order to solve the above problem, Ancuti et al. proposed another simple fusion-based defogging algorithm via another two input images also derived from the original image [118], [119]. The first input image is obtained via the white balance operation of the original foggy image, and the second input image is obtained via a simple linear transformation which is used to enhance the contrast of the foggy image. Finally, the pixel-fusion method which uses three weight maps is selected to fuse the two input images for enhancing the visibility of the foggy image. Ancuti et al. also extended their fusion-based algorithm for underwater image enhancement [55]. Their proposed fusion-based defogging algorithm is simple and fast, and can achieve similar result as physical-based defogging algorithms, such as the DCP algorithm [29] and Fattal [48]. But it fails when the image contains inhomogeneous fog. The reason is that this algorithm did not take into account the depth information of a foggy image.

Based on the fusion strategy, Fu et al. exploited two input images obtained by gamma correction with different scales

for sandstorm image enhancement [57]. Guo et al. also presented an improved fusion-based algorithm with different input images for single image defogging [56].

The fusion-based algorithm is novel and effective for single image defogging. The second input image is used to enhance the contrast of the fused image, and the first input image is used to compensate the color distortion and reduce the halo effect and noise caused by the second input image. In other words, the first image is used to restore the colors and reduce the noise, and the second image is used to enhance the visibility of the image. Although these algorithms are fast and simple, they cannot achieve good performance if the second input image cannot effectively enhance the visibility of a foggy image. Table 1 summarizes the advantages and drawbacks of some typical image defogging algorithms.

IV. VIDEO DEFOGGING ALGORITHMS

The previous image defogging algorithms have good performance on enhancing the visibility of foggy images. However, in some real-world applications, such as for scene surveillance and visual systems of an unmanned plane or vehicle, we need to enhance the real-time visibility of the video acquired by the visual system. In contrast to the various image defogging algorithms, only a few algorithms were proposed for enhancing the visibility of a video sequence in foggy weather. In addition, most video defogging algorithms were proposed for video surveillance with the same background image. But, many algorithms have been proposed for video enhancement and video denoising. Rao et al. divided the existing techniques of video denoising and night video enhancement algorithms into two categories: self-enhancement and context-based fusion enhancement [120]. The self-enhancement algorithms perform the defogging algorithm frame by frame and do not take into account the inter-frame correlation information. The context-based fusion enhancement algorithms can exploit the inter-frame correlation information. In other words, this category fuses the information of different or adjacent frames for video enhancement, which is able to preserve the color fidelity of the video. For video defogging, Guo et al. proposed two fast defogging algorithms based on the estimation of a universal foggy mask component for the surveillance scene [121]. Video defogging algorithms can be divided into three categories as shown in Fig.6. The first category is the frame-based video defogging algorithms which performs the single image defogging algorithm on each frame of the video [74], [122]. The second category is the fusion-based video defogging algorithms which is based on the fusion of the enhanced background and foreground images of each video frame. The third category of the video defogging algorithms is the universal component-based defogging algorithm which is based on the estimation of a universal component that can be used in all video frames. Performing the single image defogging algorithm on each frame is time consuming and may lead to color and brightness mutations. So in this paper, we mainly introduce the second and third category of video defogging algorithms.

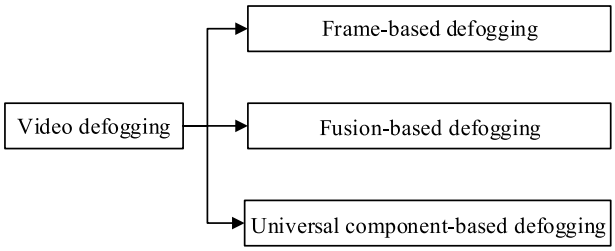

FIGURE 6. The categories of video algorithms.

Fusion-based defogging algorithms first extract the background and foreground of each frame. Then the single image defogging algorithm is used to separately enhance the background and foreground image. Finally, video defogging can be realized by fusing the enhanced background and foreground images of each frame. Fusion-based defogging algorithms restore only the background image, which allows the efficiency of the video defogging to be improved. Some researchers proposed to use the frame difference method to extract the background and foreground image of each frame and use the CLAHE algorithm to enhance the background and foreground images, respectively [8], [123]. John et al. also proposed a video defogging algorithm based on the separation of the background and foreground of the video [6]. They first used the single image defogging algorithm based on the physical model to enhance the background image and simultaneously obtained the global lightness parameter. Then the estimated lightness parameter was used to enhance the foreground image of each frame. Finally, the enhanced video was obtained via the fusion of the enhanced background image and each enhanced foreground image. We should point out that under the condition of foggy weather, the foreground image which denotes the targets is not easy to accurately extract, and the method may lead to color or brightness mutations of two adjacent frames. The reason is that single image defogging algorithms do not take into account the correlation of the color and brightness information of adjacent frames. Yoon et al. proposed an improved DCP defogging algorithm which uses the multiphase level set formulation method to replace the soft matting algorithm to restore each frame of the video, and then proposed an color correction method to solve the color mutation problem [124].

Universal component-based video defogging algorithms try to estimate a universal component which represents the fog distribution and apply it to subsequent frames of the video. These video defogging algorithms are reasonable and able to improve the efficiency. Guo et al. took the transmission of the background image of the video as the universal component for video defogging of the surveillance scene [121]. They first extracted the background of the video via the frame differential method. Then they estimated the transmission of the background image by using MSR algorithm, and used bilateral filtering and the Rudin-Osher-Fatemi (ROF) model [125] to optimize

the transmission. Finally, the universal transmission was applied to enhance the subsequent frame. Xie et al. also used the transmission of the background image of the scene as the universal component for video defogging [126]. Although taking the transmission of the background image as the universal component can greatly improve the efficiency of video defogging, some enhanced video frames especially the frames which have a large difference from the background will suffer from edge degradation and halo artifacts. The reason is that the universal transmission is estimated from the background and is not the real transmission of the subsequent video frames. Previous frames do not have the same edge information or depth information with the subsequent video frames especially the frame which has many targets, so some edges of the targets will degrade. In order to solve this problem, Ma *et al.* [127] proposed a novel fast video defogging algorithm based on the combination of guided image filtering and fog mask theory. The fog mask theory regards the fog as the mask or veil layer of the foggy image and the fog mask is obtained by subtracting the enhanced image from the original foggy image. They first used the single image defogging algorithm to enhance the first frame of the video and simultaneously obtained the fog mask. Then guided image filtering was applied to obtain the new fog masks of the subsequent frames. Finally, the enhanced video was obtained. Their video defogging algorithm does not need to extract the background, using guided image filtering to obtain the new fog mask of the corresponding new frame can effectively eliminate the 'false contour' phenomenon. So their algorithm can also be applied to a scene with a moving camera. Zhang et al. also took the transmission of the key-frame as the universal component and used the optical flow method to estimate the transmission of the non-key-frame to improve the efficiency [128].

V. OBJECTIVE QUALITY ASSESSMENT CRITERION OF THE IMAGE DEFOGGING ALGORITHM

The image quality assessment criterion can be divided into three categories: full-reference image quality assessment [129], reduced-reference image quality assessment [130], and no-reference image quality assessment [131]. The full-reference and reduced-reference image quality assessments need a clear image corresponding to the foggy image to act as the reference image. This is hard to be satisfied in real applications unless there is a synthetic foggy image. Thus, in the field of image defogging, the no-reference metric is widely used, such as peak signal-to-noise ratio (PSNR) [132], structural similarity (SSIM) [129], information entropy, average gradient, and global contrast [133].

Chen et al. presented a quality ranking system based on support vector machines (SVM) for comparing the image defogging algorithms[15] [134]. The proposed algorithm extracted 521 features of each image for training and classification. Gibson et al. also proposed a contrast enhancement metric (CEM) based on adaboost learning for foggy ocean images[16] [135]. The above two algorithms are novel but too complex.

The main purpose of image defogging is to enhance the visibility of a foggy image. A good defogging algorithm not only needs to enhance the visibility, edge, and texture information, but also to preserve the image structure and colors. An image with good visibility also means that it has obvious edge and texture information. Thus, a good image quality assessment method needs to compare the effect of visibility, color restoration, and image structure similarity of different defogging algorithms.

1) ASSESSMENT CRITERION OF IMAGE VISIBILITY

There are various indexes that can be used to compare the visibility of images, such as the first two indicators $(e, \bar{r})$ of the blind assessment [136], image visibility measurement (IVM) [37], image contrast [137], and visual contrast measure (VCM) [38].

a: BLIND ASSESSMENT INDICATOR[17]

The first two indicators $(e, \bar{r})$ of the blind assessment use the enhanced degree of image edges to represent the enhanced degree of the image visibility [136]. The first indicator e denotes the increased rate of visible edges after image defogging and is calculated by

$$e = \frac{n_r - n_o}{n_o}, \tag{31}$$

where n_r and n_o represent the cardinal numbers of the set of visible edges in restored image I_r and original image I_o, respectively. The detailed introduction of the visible edge segmentation algorithm is in references [136], [138]. The CIE defines that the set of edges which have a local contrast above 5% as visible edges [32]. Because for some images with dense fog, the number of visible edges of the original foggy image may be 0, we transformed Eq.(31) to

$$e = \frac{n_r - n_o}{M \times N}, \tag{32}$$

where M and N are the image size. The larger the e, the larger degree of visibility improvement. This indicator uses the increased number of the visible edges to represent the enhanced degree of image visibility.

The second indicator $\bar{r}$ uses the enhanced degree of image gradients to represent the restoration degree of the image edge and texture information. A larger $\bar{r}$ also means that the corresponding defogging algorithm has better edge preservation performance than others. $\bar{r}$ is calculated as

$$\bar{r} = \exp\left[\frac{1}{n_r}\sum_{i \in \wp_r} \log r_i\right], \tag{33}$$

[15]More quality assessment information of Chen are available at: http://mlg.idm.pku.edu.cn/resources/pku-eaqa.html

[16]Code and data of CEM are available at: http://videoprocessing.ucsd.edu/~kgibson/cem.htm

[17]Code and more information about the Blind assessment indicator are available at: http://perso.lcpc.fr/tarel.jean-philippe/publis/ics07.html

where $r_i = \Delta I_i^r / \Delta I_i^o$, ΔI^r, and ΔI^o are the gradient of the restored image and original image, respectively, and $\wp_r$ denotes the set of visible edges of the restored image. This gradient based index can also be used as an index to measure the restoration of edge information.

b: IMAGE VISIBILITY MEASUREMENT (IVM)

Inspired by the blind assessment indicator, Yu *et al.* [37] presented another image visibility measurement method based on the visible edge segmentation [136], [138]. The IVM is defined as

$$IVM = \frac{n_r}{n_{total}} \log \sum_{x \in \wp} C(x), \tag{34}$$

where n_r is the number of visible edges, n_{total} is the number of edges, $C(x)$ is the mean contrast, and $\wp$ denotes the image area of visible edges.

c: IMAGE CONTRAST

The contrast of a clear image is usually much higher than that of a foggy image, so image contrast can be used to compare different defogging algorithms. The higher the contrast of the enhanced image, the better the defogging algorithm. Ma and Wen [85] used the image global contrast to compare the performance of different defogging algorithms. Tripathi et al. used contrast gain to compare different defogging algorithms [42]. Contrast gain denotes the mean contrast difference between the enhanced image and original foggy image [137], and is calculated by

$$C_{gain} = \bar{C}_J - \bar{C}_I, \tag{35}$$

where $\bar{C}_J$ and $\bar{C}_I$ represent the mean contrast of the enhanced image and foggy image, respectively. For an image with size $M \times N$, its mean contrast is

$$\bar{C} = \frac{1}{MN} \sum_{y=1}^{N} \sum_{x=1}^{M} C(x, y), \tag{36}$$

where C is the local contrast of the image in a small window and is calculated by

$$C(x, y) = \frac{S(x, y)}{m(x, y)}, \tag{37}$$

where $S(x, y) = \frac{1}{(2r+1)^2} \sum_{j=-r}^{r} \sum_{i=-r}^{r} (I(x+i, y+j) - m(x, y))^2$, $m(x, y) = \frac{1}{(2r+1)^2} \sum_{j=-r}^{r} \sum_{i=-r}^{r} I(x+i, y+j)$, and r is the radius of the local area. The larger the contrast gain, the better the result of the defogging algorithm.

Ramya et al. used the contrast improvement index (CI) to compare the degree of the visibility improvement, and used the Tenengrad (Thresholded Gradient Magnitude Maximization) criterion (TEN) to evaluate the restoration effect of the edge and texture information [7]. The CI also uses the local contrast to assess the image quality. The only difference between the CI and contrast gain is the calculation of the local contrast, so the two indexes have the same effect on assessment of image quality. The TEN measures the sharpness of the image, and is calculated by the sum of the image gradient. The blind assessment indicator $\bar{r}$ can be regarded as the improved index of the TEN.

d: VISUAL CONTRAST MEASURE (VCM)

Jobson *et al.* [38] proposed a visual contrast measure (VCM) to quantify the degree of the visibility of the image and is calculated by

$$VCM = 100 * R_v / R_t, \tag{38}$$

where R_v is the number of local areas, the standard deviation of which is larger than the given threshold and R_t is the total number of local areas. Jobson et al. did not give the threshold computation algorithm. In experiments, we chose the OTSU threshold image segmentation algorithm to adaptively calculate the threshold [37], [139]. The VCM uses the local standard deviation which denotes the contrast of the image to measure the visibility. In general, the higher the VCM, the clearer the enhanced image.

2) ASSESSMENT CRITERION OF COLOR RESTORATION

The blind assessment indicator σ can be used to assess the color restoration performance of defogging algorithms [136]. σ denotes the rate of the saturated pixels after image defogging and is calculated as

$$\sigma = \frac{n_s}{M \times N}, \tag{39}$$

where M and N are the size of the image and n_s denotes the number of black and white pixels of the enhanced image which are not absolutely black and white in the original fog image. The smaller the σ, the better the result of the defogging algorithm. But we should point out that indictor σ is not perfect in comparing different algorithms. This is because the enhanced image of some algorithms especially the Retinex-based algorithms need to be transformed into the display domain [0, 255] via the gain/offset algorithm. The gain/offset algorithm will transform some pixels to black and white pixels to improve the dynamic range for display, which leads to a high σ.

Yu et al. thought that a good defogging algorithm should allow the original foggy image and enhanced image to have similar Histogram distributions [61]. They used the Histogram correlation coefficient (HCC) of the two color images as the criterion to assess the performance of color restoration.

3) IMAGE STRUCTURE SIMILARITY

Wu and Zhu [41] used the image structural similarity (SSIM) and universal quality index (UQI) [140] to assess the performance of the structural similarity between the original foggy image and the enhanced image. The traditional SSIM and UQI criterions both use an image with high quality as the reference image. Thus, the higher the SSIM and UQI,

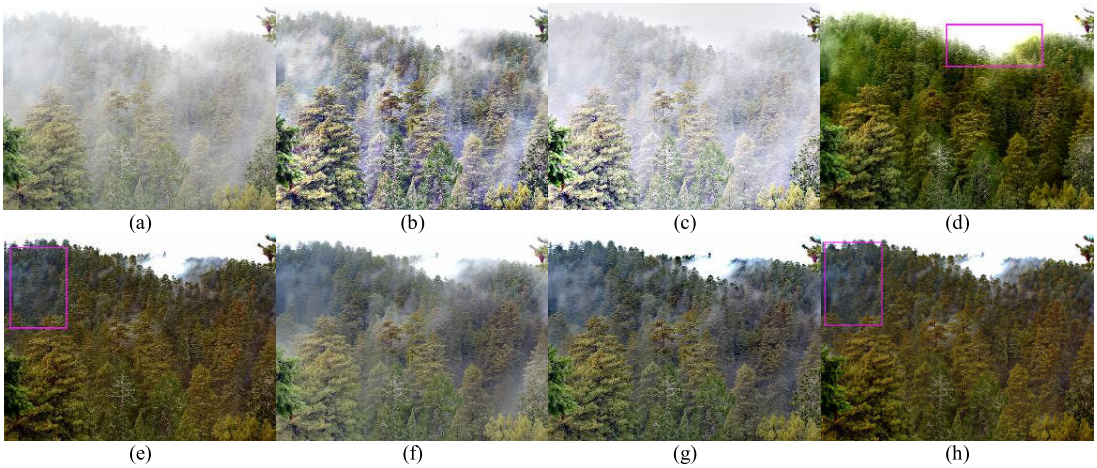

FIGURE 7. Comparisons of some classical defogging algorithms with an inhomogeneous fog scene. (a) original image. (b) CLAHE [108]. (c) MSRCR [98]. (d) Fattal [48]. (e) Tarel and Hautiere [19]. (f) He *et al.* [29]. (g) Meng *et al.* [81]. (h) Ancuti *et al.* [31].

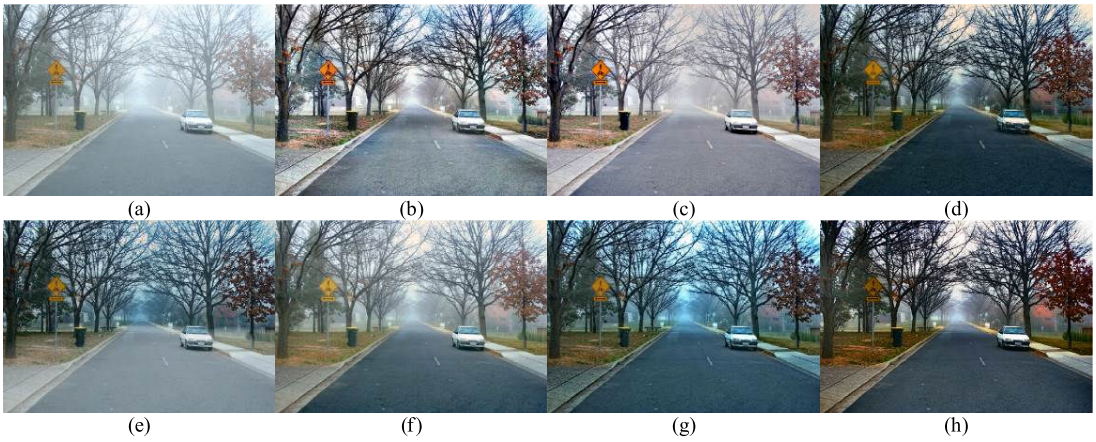

FIGURE 8. Comparisons of some classical defogging algorithms with a road scene. (a) original image. (b) CLAHE [108]. (c) MSRCR [98]. (d) Fattal [48]. (e) Tarel and Hautiere [19]. (f) He *et al.* [29]. (g) Meng *et al.* [81]. (h) Ancuti *et al.* [31].

the better the compared image. However, in real-world applications of image defogging, the original foggy image is always chosen as the reference image, so large SSIM and UQI do not means the image is of high quality. For example, the SSIM index of two identical foggy images must be larger than the SSIM index of the foggy image and the enhanced image. So the enhanced image with the best visibility may have the smallest SSIM and UQI. Also, the removal of fog from a foggy image will also change the image structure. This also leads to a small SSIM and UQI.

VI. EXPERIMENTS

In this section, some classical single image defogging algorithms were compared via subjective and objective assessment. Fig.7-Fig.9 show the image defogging results. In the experiment, two classical image enhancement algorithms, four physical model-based defogging algorithms, and a fusion-based defogging algorithm were compared. Nine objective quality assessment indexes were used to compare these classical defogging algorithms. Table 1-Table 3 show the quality comparison of these classical defogging algorithms.

Fig.7-Fig.10 show that the MSRCR algorithm achieved the best performance in preserving the colors, but it does not effectively enhance the visibility. The CLAHE algorithm is a simple and effective algorithm for enhancing dark and homogeneous foggy images (see Fig.8(b) and Fig.9(b)), but it fails to enhance inhomogeneous foggy images (see Fig.7(b)). This also demonstrates that the simple CLAHE algorithm cannot solve the depth discontinuous problem. The defogging algorithm proposed by Meng et al is an improved algorithm of He et al., so their defogging results were better than He et al. (see Fig.7(g) and Fig.8(g)), but it caused color distortion (see Fig.9(g)) owing to the error estimation of the atmospheric light. The defogging algorithms of Fattal, Tarel et al., and Ancuti et al. greatly enhanced the visibility of foggy images. The defogging algorithm of Fattal achieved the best performance on removing inhomogeneous fog, but some

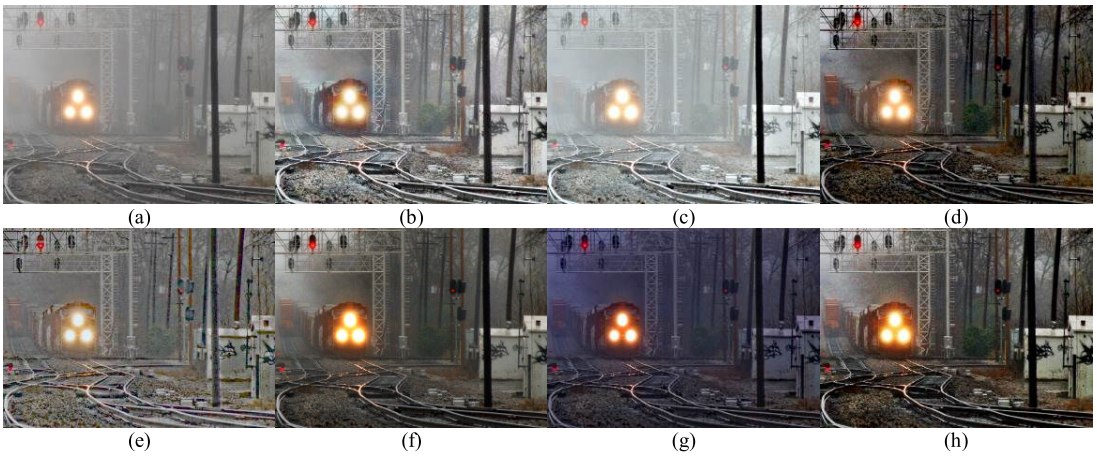

FIGURE 9. Comparisons of some classical defogging algorithms with a dark and foggy scene. (a) original image. (b) CLAHE [108]. (c) MSRCR [98]. (d) Fattal [48]. (e) Tarel and Hautiere [19]. (f) He *et al.* [29]. (g) Meng *et al.* [81]. (h) Ancuti *et al.* [31].

TABLE 2. The objective image quality comparison of defogging results of Fig.7.

Quality assessment	CLAHE	MSRCR	Fattal	Tarel et al.	He et al.	Meng et al.	Ancuti et al.
e	18.667	3.2592	12.792	**26.914**	15.449	15.583	20.403
$\overline{r}$	**2.8449**	1.7413	2.4547	2.1579	1.5645	2.1796	2.0887
IVM	9.3588	6.2581	**10.647**	10.523	8.9027	10.268	10.374
Contrast gain	0.2897	0.0767	**0.8571**	0.7636	0.2024	0.4928	0.7257
VCM	81.429	48.929	**85.893**	72.6786	54.821	76.964	79.643
σ	0.0045	0.0095	0.1323	0.0057	0.0057	0.0082	**0.0032**
HCC	0.1187	0.2072	-0.0971	0.4995	**0.6464**	0.5716	-0.1917
SSIM	0.6942	0.8983	**0.4916**	0.5350	0.8088	0.6782	0.5549
UQI	0.9561	0.9710	0.5401	**0.4882**	0.8376	0.6959	0.5076

TABLE 3. The objective image quality comparison of defogging results of Fig.8.

Quality assessment	CLAHE	MSRCR	Fattal	Tarel et al.	He et al.	Meng et al.	Ancuti et al.
e	11.5204	6.0342	13.3971	6.4796	9.9617	13.153	**21.168**
$\overline{r}$	**2.7109**	1.8737	2.0530	1.9894	1.4310	2.1209	2.2358
IVM	8.3440	6.6577	9.7656	6.6515	6.9121	8.7626	**9.8866**
Contrast gain	0.3557	0.2355	**0.5455**	0.3346	0.1341	0.4363	0.5176
VCM	**75.667**	67.333	66.667	63	59	67	69.333
σ	0.0011	0.0142	0.0015	**0**	**0**	0.0004	0.0002
HCC	**0.8277**	0.8021	-0.5212	0.5950	0.2294	-0.3295	-0.5128
SSIM	0.6966	0.8673	**0.5862**	0.7666	0.8997	0.6785	0.6063
UQI	0.9017	0.9554	**0.5300**	0.8005	0.8929	0.6762	0.5992

scenes were also removed as shown in the 'box' area of Fig.7(d). Fig.8(d) and Fig.9(d) show that the defogging results of Fattal had low brightness. A better result may be obtained by further enhancing its brightness via the white balance operation or gamma correction.

The above tables show that the MSRCR algorithm achieved smaller values of all visibility assessment criteria than other defogging algorithms. This is consistent with the subjective assessment. The above tables also demonstrate that all the above defogging algorithms were able to improve the visibility of the foggy image. Specially, the improved DCP algorithm of Meng achieved larger values of all visibility criteria than the defogging algorithm of He, which is consistent with the comparisons of the defogging results. The above tables show that the defogging algorithm of Ancuti achieved a larger e than other defogging algorithms, which demonstrate that the algorithm had the best performance in restoring image edges. The defogging algorithm of Fattal achieved better contrast restoration performance than the other algorithms.

Compared to the corresponding original image, the results of Fattal, Meng, and Ancuti shown in Fig.8 and Fig.9 had the problem of color distortion. The HCC values shown in Table 3 and Table 4 of their algorithms prove that the HCC criterion is consistent with the subjective assessment and can be used as the criterion for the comparison of color

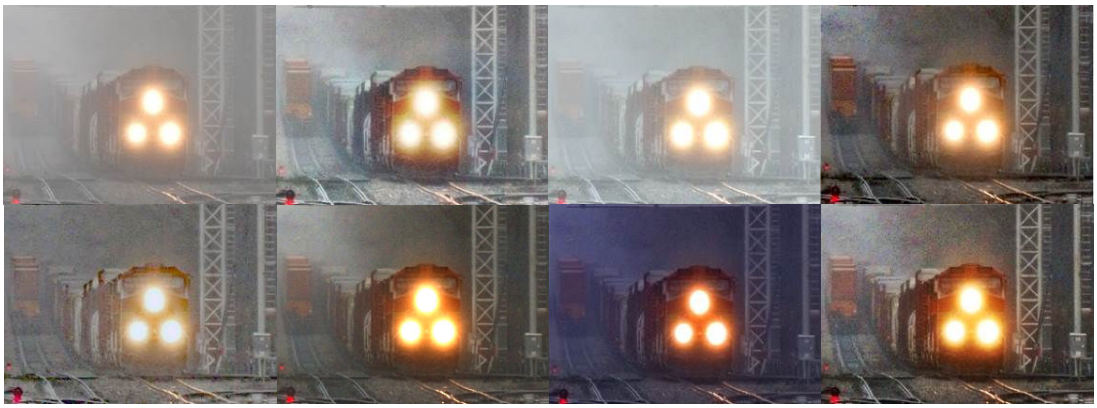

FIGURE 10. Local areas of corresponding image in Fig.9.

TABLE 4. The objective image quality comparison of defogging results of Fig.9.

Quality assessment	CLAHE	MSRCR	Fattal	Tarel et al.	He et al.	Meng et al.	Ancuti et al.
e	20.104	3.629	21.9458	17.668	22.2475	22.655	**25.286**
$\overline{r}$	2.9862	1.896	3.1256	**3.2471**	1.9155	1.5660	2.9284
IVM	7.7773	4.3465	**10.566**	8.7370	8.4181	8.5718	10.0961
Contrast gain	0.2780	0.1363	**1.1631**	0.4033	0.3827	0.4588	0.7608
VCM	77.667	45.167	**80**	73.833	55	41.333	78.833
σ	0.0009	0.0141	0.0661	**0.0006**	0.0045	0.0033	0.0451
HCC	**0.9123**	0.1591	-0.0913	0.5328	-0.0370	-0.2210	-0.0185
SSIM	0.7049	0.8680	**0.5546**	0.6964	0.7578	0.6807	0.5744
UQI	0.9608	0.9196	0.5942	0.9209	0.7303	**0.5201**	0.6751

FIGURE 11. Results of some defogging algorithms on an aerial photo without a sky area. (a) original image. (b) CLAHE [108]. (c) MSRCR [98]. (d) Tarel and Hautiere [19]. (e) Meng *et al.* [81]. (f) Nishino *et al.* [82].

restoration of different defogging algorithms. The above tables and figures also prove that the HCC criterion is better than the third blind assessment indicator σ for the comparison of color restoration of different defogging algorithms.

Table 2-Table 4 demonstrate that physical model-based algorithms preserve better image structure than enhanced-based and fusion-based defogging algorithms. The above tables and figures prove that the smaller the SSIM and UQI indexes, the better the defogging result. This also proves that the removal of fog from an image will also change the image structure.

There is no defogging algorithm that had very good performance under all conditions, so it is hard to determine which algorithm is the best defogging algorithm. From the above tables and figures, it can be seen that the quality assessment indexes are not absolutely consistent with the subjective assessment, but they can be used as references for comparing different defogging algorithms.

Some defogging algorithms are chosen for single image defogging under different conditions, such as on the sea or without sky area, and dense fog or thin fog. The defogging results are shown in Fig.11-Fig.15. Fig.11-Fig.15 show that the MSRCR algorithm achieved good performance in enhancing sea fog images. For sea fog images, the algorithm of Meng was not suitable. Fig.12 shows that the algorithm of Nishino was robust to the image with high brightness, but the algorithm caused color distortion. Fig.13 shows that the algorithm of Tarel greatly enhanced the road image with dense fog. In Fig.13-Fig.15, the transmission of the He algorithm [29] was optimized by fast guided image filtering [141]. Table 5 shows the comparison of the computation efficiency of some typical defogging algorithms. From Table 5, we can see that Meng's algorithm needs more computation time than the defogging algorithm of He. This also demonstrates that to iteratively calculate the transmission image is time consuming.

FIGURE 12. Results of some defogging algorithms on a road scene with high brightness. (a) original image. (b) CLAHE [108]. (c) MSRCR [98]. (d) Tarel and Hautiere [19]. (e) Meng *et al.* [81]. (f) Nishino *et al.* [82].

FIGURE 13. Results of some defogging algorithms on a road scene with dense fog. (a) original image. (b) CLAHE [108]. (c) MSRCR [98]. (d) Tarel and Hautiere [19]. (e) He *et al.* [29]. (f) Meng *et al.* [81].

FIGURE 14. Results of some defogging algorithms on a sea scene with dense fog. (a) original image. (b) CLAHE [108]. (c) MSRCR [98]. (d) Tarel and Hautiere [19]. (e) He *et al.* [29]. (f) Meng *et al.* [81].

FIGURE 15. Results of some defogging algorithms on a sea scene with thin fog. (a) original image. (b) CLAHE [108]. (c) MSRCR [98]. (d) Tarel and Hautiere [19]. (e) Heet *al.* [29]. (f) Meng *et al.* [81].

TABLE 5. The computation time (s) of some typical defogging algorithms.

Original foggy image	size	CLAHE	MSRCR	Tarel	He	Meng
Fig.13	236*158	0.0739	0.0674	0.2062	0.1771	0.4035
Fig.14	800*536	0.1127	0.3398	17.4432	1.1087	3.2339
Fig.15	833*546	0.1158	0.4328	19.5508	1.1960	3.4927

Note: above algorithms are tested on the same computer. The system is Win 7, and the software is Matlab 2015a. The hardware is Intel Core i7-4790 CPU and 16 GB RAM.

TABLE 6. Defogging time (s) of different improved dark channel prior algorithms based on using different transmission methods.

Original image	size	Soft matting	Bilateral filtering	Joint bilateral filtering	Guided image filtering	Meng
Fig.16	600*450	117.18	6.66	9.1164	0.7096	1.9382

The dark channel prior based defogging algorithm is one of the most popular single image defogging algorithm in recent years. To improve the edge preservation and efficiency, various transmission optimization algorithms have been proposed. Thus, we compare some typical transmission optimization algorithms in this experiment. Fig.16 and Table 6

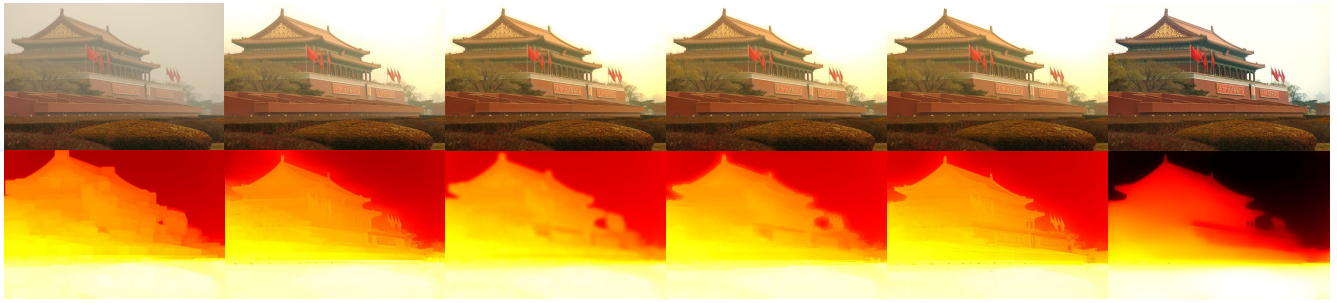

FIGURE 16. Comparison of some improved dark channel prior based defogging algorithms based on different transmission optimization methods. Images in the first row are the original foggy image and defogging results obtained using the optimization of soft matting [29], bilateral filtering [77], joint bilateral filtering [78], guided image filtering [30] and Meng's optimization algorithm [81], respectively. Images in the second rows are original transmission image and the optimized transmission image obtained using the above algorithms, respectively.

show the comparison of some typical improved dark channel prior based defogging algorithms. We see that the soft matting algorithm, bilateral filtering, joint bilateral filtering and guided image filtering algorithm obtained close results, but using guided image filtering can greatly improve the efficiency.

VII. CONCLUSIONS

This paper not only summarizes various video and image defogging algorithms, but also gives a brief introduction of related image restoration and enhancement methods. Although single image defogging algorithms have received significant development in past years, there are still many problems which need to be addressed. In addition, video defogging algorithms are the key technology for realizing the goal of intelligent defogging, but also many difficulties have to be overcome. The main problems are as follows:

1) Few technologies can judge whether the current scene has fog or not. The existing defogging algorithms only have the ability to restore a foggy image. So it is important to overcome this problem in the future. The fog level classification of the foggy image is also worth studying. It is able to improve the estimation of some parameters for image defogging. In past years, many pattern recognition algorithms have been proposed, especially deep learning based classification methods. The deep learning method does not need humans to find the most difference features of the foggy images and clear images. It can automatically extract the discriminative features from images and learn a model for classification.
2) There is no single image defogging algorithm that can obtain good performance in all kinds of foggy weather. Existing single image defogging algorithms can effectively enhance an image with homogenous fog or thin fog. However, if the fog is unevenly distributed in an image or an image is full of dense fog, some single image defogging algorithms will fail. So it is necessary to further study single image defogging algorithms that are able to adaptively enhance a foggy image acquired under different foggy weather, such as night foggy weather, dense foggy weather, and inhomogeneous foggy weather. Maybe we can integrate foggy image classification, visibility detection, and single image defogging to solve this problem. Some existing algorithms especially defogging algorithms based on the imaging physical model under foggy weather focus on land foggy images. This imaging model may be not the perfect model for other scenes, such as on the sea or in the air. So it is necessary to establish a more appropriate model or multiple models for various scenes. The fusion-based defogging algorithm may be a potential approach to address these problems. For some special scenes, we can fuse two defogging images obtained using two different defogging algorithms.
3) In some of the existing defogging algorithms, parameters need to be set manually. Although a good performance can be obtained by constantly adjusting its parameters, this is unrealistic in real-time applications. Simple, fast, and effective algorithms are necessary. The parameters can be adaptively set in terms of the fog level of images. This also demonstrates that classification of the fog level of images is very important.
4) Video defogging algorithms are an important technology in the visual system. However, all the existing video defogging algorithms focus on a surveillance scene. There are no effective video defogging algorithms for a scene with a moving camera. For video defogging, effectiveness and real-time processing are equally important. It is difficult to simultaneously ensure good defogging results and real-time processing. For some existing video defogging algorithms based on background extraction, the background estimation has a great influence on the result of video defogging. Thus, to find a good and fast background estimation algorithm under foggy weather is necessary. The color shift problem also needs to be overcome in further study. For a moving camera such as vehicle traveling data recorder, the frame-based video defogging algorithms and universal component-based defogging

algorithms should be more suitable. For real-time scenarios, maybe we can sacrifice a little image restoration quality to improve the efficiency.

5) As previous objective assessment is not absolutely consistent with the subjective assessment, it is hard to be directly applied to evaluate different defogging algorithms. Thus, a better quality assessment index or method also needs to be proposed. Maybe some intelligent machine learning algorithms such as the deep learning algorithm can be introduced for image quality assessment.

ACKNOWLEDGMENT

The authors would like to thank Dr. Edward C. Mignot, Shandong University, for linguistic advice.

REFERENCES

[1] R. Sharma and V. Chopra, "A review on different image dehazing methods," *Int. J. Comput. Eng. Appl.*, vol. 6, no. 3, pp. 77–87, Jun. 2014.

[2] N. Hautière, J.-P. Tarel, and D. Aubert, "Towards fog-free in-vehicle vision systems through contrast restoration," in *Proc. IEEE Conf. Comput. Vis. Pattern Recognit. (CVPR)*, Jun. 2007, pp. 1–8.

[3] S. G. Narasimhan, C. Wang, and S. K. Nayar, "All the images of an outdoor scene," in *Computer Vision* (Lecture Notes in Computer Science), vol. 2352. Heidelberg, Germany: Springer, 2002, pp. 148–162.

[4] S. G. Narasimhan and S. K. Nayar, "Vision and the atmosphere," *Int. J. Comput. Vis.*, vol. 48, no. 3, pp. 233–254, 2002.

[5] S. G. Narasimhan and S. K. Nayar, "Removing weather effects from monochrome images," in *Proc. IEEE Comput. Soc. Conf. Comput. Vis. Pattern Recognit. (CVPR)*, vol. 2. Dec. 2001, pp. II-186–II-193.

[6] J. John and M. Wilscy, "Enhancement of weather degraded video sequences using wavelet fusion," in *Proc. 7th IEEE Int. Conf. Cybern. Intell. Syst.*, Sep. 2008, pp. 1–6.

[7] C. Ramya and D. S. S. Rani, "Contrast enhancement for fog degraded video sequences using BPDFHE," *Int. J. Comput. Sci. Inf. Technol.*, vol. 3, no. 2, pp. 3463–3468, 2012.

[8] Z. Xu, X. Liu, and X. Chen, "Fog removal from video sequences using contrast limited adaptive histogram equalization," in *Proc. IEEE Int. Conf. Comput. Intell. Softw. Eng.*, Dec. 2009, pp. 1–4.

[9] Z. Lin and X. Wang, "Dehazing for image and video using guided filter," *Open J. Appl. Sci.*, vol. 2, no. 4B, pp. 123–127, 2012.

[10] Z. Ma, J. Wen, and X. Liang, "Video image clarity algorithm research of USV visual system under the sea fog," in *Advances in Swarm Intelligence* (Lecture Notes in Computer Science), vol. 7929. Heidelberg, Germany: Springer, 2013, pp. 436–444.

[11] G. S. Rajput and Z.-U. Rahman, "Hazard detection on runways using image processing techniques," in *Proc. SPIE*, Apr. 2008, pp. 69570D-1–69570D-12.

[12] D. J. Jobson, Z.-U. Rahman, and G. A. Woodell, "Retinex image processing: Improved fidelity to direct visual observation," in *Proc. Color Imag. Conf.*, Jan. 1996, pp. 124–125.

[13] Z.-U. Rahman, D. J. Jobson, and G. A. Woodell, "Multiscale retinex for color rendition and dynamic range compression," in *Proc. SPIE*, Nov. 1996, pp. 183–191.

[14] Z.-U. Rahman, G. A. Woodell, and D. J. Jobson, "A comparison of the multiscale retinex with other image enhancement techniques," in *Proc. IS&T 50th Anniversary Conf.*, May 1997, pp. 1–6.

[15] Z.-U. Rahman, D. J. Jobson, G. A. Woodell, and G. D. Hines, "Image enhancement, image quality, and noise," in *Proc. SPIE*, Sep. 2005, pp. 59070N-1–59070N-15.

[16] G. D. Hines, Z.-U. Rahman, D. J. Jobson, and G. A. Woodell, "Realtime enhancement, registration, and fusion for a multisensor enhanced vision system," in *Proc. SPIE*, May 2006, pp. 622609-1–622609-8.

[17] L. Caraffa and J.-P. Tarel, "Stereo reconstruction and contrast restoration in daytime fog," in *Computer Vision* (Lecture Notes in Computer Science), vol. 7727. Heidelberg, Germany: Springer, 2013, pp. 13–25.

[18] N. Hautière, J.-P. Tarel, and D. Aubert, "Simultaneous contrast restoration and obstacles detection: First results," in *Proc. IEEE Intell. Vehicles Symp.*, Jun. 2007, pp. 130–135.

[19] J.-P. Tarel and N. Hautière, "Fast visibility restoration from a single color or gray level image," in *Proc. IEEE 12th Int. Conf. Comput. Vis.*, Sep./Oct. 2009, pp. 2201–2208.

[20] K. Garg and S. K. Nayar, "Detection and removal of rain from videos," in *Proc. IEEE Conf. Comput. Vis. Pattern Recognit. (CVPR)*, vol. 1. Jun./Jul. 2004, pp. I-528–I-535.

[21] S. G. Narasimhan and S. K. Nayar, "Chromatic framework for vision in bad weather," in *Proc. IEEE Conf. Comput. Vis. Pattern Recognit. (CVPR)*, vol. 1. Jun. 2000, pp. 598–605.

[22] S. G. Narasimhan and S. K. Nayar, "Contrast restoration of weather degraded images," *IEEE Trans. Pattern Anal. Mach. Learn.*, vol. 25, no. 6, pp. 713–724, Jun. 2003.

[23] S. G. Narasimhan and S. K. Nayar, "Interactive (de)weathering of an image using physical models," in *Proc. IEEE Workshop Color Photometric Methods Comput. Vis.*, vol. 6. Oct. 2003, pp. 1–8.

[24] E. Namer and Y. Y. Schechner, "Advanced visibility improvement based on polarization filtered images," in *Proc. SPIE*, Sep. 2005, pp. 588805-1–588805-10.

[25] Y. Y. Schechner and Y. Averbuch, "Regularized image recovery in scattering media," *IEEE Trans. Pattern Anal. Mach. Intell.*, vol. 29, no. 9, pp. 1655–1660, Sep. 2007.

[26] Y. Y. Schechner, S. G. Narasimhan, and S. K. Nayar, "Polarization-based vision through haze," *Appl. Opt.*, vol. 42, no. 3, pp. 511–525, Jan. 2003.

[27] S. Shwartz, E. Namer, and Y. Y. Schechner, "Blind haze separation," in *Proc. IEEE Comput. Soc. Conf. Comput. Vis. Pattern Recognit. (CVPR)*, vol. 2. Jun. 2006, pp. 1984–1991.

[28] Y. Y. Schechner, S. G. Narasimhan, and S. K. Nayar, "Instant dehazing of images using polarization," in *Proc. IEEE Comput. Soc. Conf. Comput. Vis. Pattern Recognit. (CVPR)*, vol. 1. Dec. 2001, pp. I-325–I-332.

[29] K. He, J. Sun, and X. Tang, "Single image haze removal using dark channel prior," *IEEE Trans. Pattern Anal. Mach. Intell.*, vol. 33, no. 12, pp. 2341–2353, Dec. 2011.

[30] K. He, J. Sun, and X. Tang, "Guided image filtering," *IEEE Trans. Pattern Anal. Mach. Intell.*, vol. 35, no. 6, pp. 1397–1409, Jun. 2013.

[31] C. O. Ancuti, C. Ancuti, C. Hermans, and P. Bekaert, "A fast semi-inverse approach to detect and remove the haze from a single image," in *Computer Vision* (Lecture Notes in Computer Science), vol. 6493. Heidelberg, Germany: Springer, 2011, pp. 501–514.

[32] *International Lighting Vocabulary*, Central Bureau Commission Int. l'Eclairage, Vienna, Austria, 1989.

[33] N. Hautière, R. Labayrade, C. Boussard, J.-P. Tarel, and D. Aubert, "Perception through scattering media for autonomous vehicles," in *Autonomous Robots Research Advances*. Hauppauge, NY, USA: Nova Science Publishers, Inc., 2008, pp. 223–267.

[34] N. Hautière, J.-P. Tarel, J. Lavenant, and D. Aubert, "Automatic fog detection and estimation of visibility distance through use of an onboard camera," *Mach. Vis. Appl.*, vol. 17, no. 1, pp. 8–20, Apr. 2006.

[35] S. Bronte, L. M. Bergasa, and P. F. Alcantarilla, "Fog detection system based on computer vision techniques," in *Proc. IEEE Conf. Intell. Transp. Syst.*, Oct. 2009, pp. 1–6.

[36] G. Li, J.-F. Wu, and Z.-Y. Lei, "Research progress of image haze grade evaluation and dehazing technology," (in Chinese), *Laser J.*, vol. 35, no. 9, pp. 1–6, Sep. 2014.

[37] X. Yu, C. Xiao, M. Deng, and L. Peng, "A classification algorithm to distinguish image as haze or non-haze," in *Proc. IEEE Int. Conf. Image Graph.*, Aug. 2011, pp. 286–289.

[38] D. J. Jobson, Z.-U. Rahman, G. A. Woodell, and G. D. Hines, "A comparison of visual statistics for the image enhancement of FORESITE aerial images with those of major image classes," in *Proc. SPIE*, May 2006, pp. 624601-1–624601-8.

[39] Y. Zhang, G. Sun, Q. Ren, and D. Zhao, "Foggy images classification based on features extraction and SVM," in *Proc. Int. Conf. Softw. Eng. Comput. Sci.*, Sep. 2013, pp. 142–145.

[40] M. Pavlic, H. Belzner, G. Rigoll, and S. Ilic, "Image based fog detection in vehicles," in *Proc. IEEE Conf. Intell. Vehicles Symp.*, Jun. 2012, pp. 1132–1137.

[41] D. Wu and Q.-S. Zhu, "The latest research progress of image dehazing," (in Chinese), *Acta Automatica Sinica*, vol. 41, no. 2, pp. 221–239, Feb. 2015.

[42] A. K. Tripathi and S. Mukhopadhyay, "Removal of fog from images: A review," *IETE Tech. Rev.*, vol. 29, no. 2, pp. 148–156, Apr. 2012.

[43] G. Yadav, S. Maheshwari, and A. Agarwal, "Fog removal techniques from images: A comparative review and future directions," in *Proc. Int. Conf. Signal Propag. Comput. Technol.*, Jul. 2014, pp. 44–52.

[44] D. Shrivastava and B. Chourasia, "An extensive survey on image defogging techniques," *Int. J. Innov. Trends Eng.*, vol. 3, no. 1, pp. 1–6, 2015.
[45] H. Kaur and R. Mahajan, "A review on various visibility restoration techniques," *Int. J. Adv. Res. Comput. Commun. Eng.*, vol. 3, no. 5, pp. 6572–6576, May 2014.
[46] K. B. Gibson, D. T. Vo, and T. Q. Nguyen, "An investigation of dehazing effects on image and video coding," *IEEE Trans. Image Process.*, vol. 21, no. 2, pp. 662–673, Feb. 2012.
[47] S.-C. Huang, B.-H. Chen, and W.-J. Wang, "Visibility restoration of single hazy images captured in real-world weather conditions," *IEEE Trans. Circuits Syst. Video Technol.*, vol. 24, no. 10, pp. 1814–1824, Oct. 2014.
[48] R. Fattal, "Single image dehazing," *ACM Trans. Graph.*, vol. 27, no. 3, pp. 72:1–72:10, Aug. 2008.
[49] M. Wang, S.-D. Zhou, F. Huang, Z.-H. Liu, and H. Bai, "The study of color image defogging based on wavelet transform and single scale retinex," in *Proc. SPIE*, Jun. 2011, pp. 81940F-1–81940F-7.
[50] B.-N. Yu, B.-S. Kim, and K.-H. Lee, "Visibility enhancement based real—Time retinex for diverse environments," in *Proc. 8th Int. Conf. Signal Image Technol. Internet Based Syst.*, Nov. 2012, pp. 72–79.
[51] L. Li, W. Jin, C. Xu, and X. Wang, "Color image enhancement using nonlinear sub-block overlapping local equilibrium algorithm under fog and haze weather conditions," (in Chinese), *Trans. Beijing Inst. Technol.*, vol. 33, no. 5, pp. 516–522, May 2013.
[52] Y. Qu, "Study of removing fog from images based on moving mask," (in Chinese), *Comput. Eng. Appl.*, vol. 49, no. 24, pp. 186–190, 2013.
[53] Y. Wang and C. Fan, "Single image defogging by multiscale depth fusion," *IEEE Trans. Image Process.*, vol. 23, no. 11, pp. 4826–4837, Nov. 2014.
[54] X. Zhao, R. Wang, and Y. Qiu, "An enhancement method of fog-degraded images," in *Proc. SPIE*, Feb. 2010, pp. 75461S-1–75461S-6.
[55] C. Ancuti, C. O. Ancuti, T. Haber, and P. Bekaert, "Enhancing underwater images and videos by fusion," in *Proc. IEEE Conf. Comput. Vis. Pattern Recognit. (CVPR)*, Jun. 2012, pp. 81–88.
[56] F. Guo, J. Tang, and Z. Cai, "Fusion strategy for single image dehazing," *Int. J. Digit. Content Technol. Appl.*, vol. 7, no. 1, pp. 19–28, Jan. 2013.
[57] X. Fu, Y. Huang, D. Zeng, X.-P. Zhang, and X. Ding, "A fusion-based enhancing approach for single sandstorm image," in *Proc. IEEE Int. Workshop Multimedia Signal Process.*, Sep. 2014, pp. 1–5.
[58] L. Schaul, C. Fredembach, and S. Süsstrunk, "Color image dehazing using the near-infrared," in *Proc. IEEE Int. Conf. Image Process.*, Nov. 2009, pp. 1–4.
[59] E. J. McCartney, *Optics of the Atmosphere: Scattering by Molecules and Particles*. New York, NY, USA: Wiley, 1976.
[60] S. K. Nayar and S. G. Narasimhan, "Vision in bad weather," in *Proc. IEEE Conf. Comput. Vis.*, vol. 2. Sep. 1999, pp. 820–827.
[61] J. Yu, D. Xu, and Q. Liao, "Image defogging: A survey," (in Chinese), *J. Image Graph.*, vol. 16, no. 9, pp. 1561–1576, 2011.
[62] F. Guo, Z.-X. Cai, B. Xie, and J. Tang, "Review and prospect of image dehazing techniques," (in Chinese), *J. Comput. Appl.*, vol. 30, no. 9, pp. 2417–2421, Nov. 2010.
[63] D. Miyazaki, D. Akiyama, M. Baba, R. Furukawa, S. Hiura, and N. Asada, "Polarization-based dehazing using two reference objects," in *Proc. IEEE Int. Conf. Comput. Vis. Workshops*, Dec. 2013, pp. 852–859.
[64] T. Treibitz and Y. Y. Schechner, "Polarization: Beneficial for visibility enhancement?" in *Proc. IEEE Conf. Comput. Vis. Pattern Recognit.*, Jun. 2009, pp. 525–532.
[65] L. Kratz and K. Nishino, "Factorizing scene albedo and depth from a single foggy image," in *Proc. IEEE 12th Conf. Comput. Vis.*, Sep./Oct. 2009, pp. 1701–1708.
[66] S. Fang, J. Zhan, Y. Cao, and R. Rao, "Improved single image dehazing using segmentation," in *Proc. 17th IEEE Int. Conf. Image Process.*, Sep. 2010, pp. 3589–3592.
[67] F. Guo, H. Peng, and J. Tang, "A new restoration algorithm for single image defogging," in *Pattern Recognition*. Heidelberg, Germany: Springer, 2014, pp. 169–178.
[68] Y. Lee, K. B. Gibson, Z. Lee, and T. Q. Nguyen, "Stereo image defogging," in *Proc. IEEE Int. Conf. Image Process.*, Oct. 2014, pp. 5427–5431.
[69] A. Hyvärinen and E. Oja, "Independent component analysis: Algorithms and applications," *Neural Netw.*, vol. 13, nos. 4–5, pp. 411–430, Jun. 2000.
[70] P. Pérez, "Markov random fields and images," *CWI Quart.*, vol. 11, no. 4, pp. 413–437, Apr. 1998.
[71] R. T. Tan, "Visibility in bad weather from a single image," in *Proc. IEEE Conf. Comput. Vis. Pattern Recognit.*, Jun. 2008, pp. 1–8.
[72] K. B. Gibson and T. Q. Nguyen, "On the effectiveness of the dark channel prior for single image dehazing by approximating with minimum volume ellipsoids," in *Proc. Int. Conf. Acoust., Speech Signal Process.*, vol. 1. May 2011, pp. 1253–1256.
[73] B. Xie, F. Guo, and Z. Cai, "Improved single image dehazing using dark channel prior and multi-scale retinex," in *Proc. Int. Conf. Intell. Syst. Design Eng. Appl.*, Oct. 2010, pp. 848–851.
[74] K. Gibson, D. Vo, and T. Nguyen, "An investigation in dehazing compressed images and video," in *Proc. OCEANS*, Sep. 2010, pp. 1–8.
[75] D. Park, D. K. Han, and H. Ko, "Single image haze removal with WLS-based edge-preserving smoothing filter," in *Proc. IEEE Int. Conf. Acoust., Speech Signal Process.*, May 2013, pp. 2469–2473.
[76] K. B. Gibson and T. Q. Nguyen, "Fast single image fog removal using the adaptive Wiener filter," in *Proc. IEEE Int. Conf. Image Process.*, Sep. 2013, pp. 714–718.
[77] J. Yu, C. Xiao, and D. Li, "Physics-based fast single image fog removal," in *Proc. IEEE 10th Int. Conf. Signal Process. (ICSP)*, Oct. 2010, pp. 1048–1052.
[78] C. Xiao and J. Gan, "Fast image dehazing using guided joint bilateral filter," *Vis. Comput.*, vol. 28, nos. 6–8, pp. 713–721, Jun. 2012.
[79] S.-C. Pei and T.-Y. Lee, "Nighttime haze removal using color transfer preprocessing and dark channel prior," in *Proc. 19th IEEE Int. Conf. Image Process.*, Sep./Oct. 2012, pp. 957–960.
[80] C. Feng, S. Zhuo, X. Zhang, L. Shen, and S. Süsstrunk, "Near-infrared guided color image dehazing," in *Proc. IEEE Int. Conf. Image Process.*, Sep. 2013, pp. 2363–2367.
[81] G. Meng, Y. Wang, J. Duan, S. Xiang, and C. Pan, "Efficient image dehazing with boundary constraint and contextual regularization," in *Proc. IEEE Int. Conf. Comput. Vis.*, Dec. 2013, pp. 617–624.
[82] K. Nishino, L. Kratz, and S. Lombardi, "Bayesian defogging," *Int. J. Comput. Vis.*, vol. 98, no. 3, pp. 263–278, Jul. 2012.
[83] K. Tang, J. Yang, and J. Wang, "Investigating haze-relevant features in a learning framework for image dehazing," in *Proc. IEEE Conf. Comput. Vis. Pattern Recognit.*, Jun. 2014, pp. 2995–3002.
[84] E. H. Land and J. J. McCann, "Lightness and retinex theory," *J. Opt. Soc. Amer.*, vol. 61, no. 1, pp. 1–11, Jan. 1971.
[85] Z. Ma and W. Jie, "Single-scale retinex sea fog removal algorithm fused the edge information," *J. Comput.-Aided Design Comput. Graph.*, vol. 27, no. 2, pp. 217–225, 2015.
[86] Z.-U. Rahman, D. J. Jobson, and G. A. Woodell, "Retinex processing for automatic image enhancement," *J. Electron. Imag.*, vol. 13, no. 1, pp. 100–110, Jan. 2004.
[87] Z.-U. Rahman, D. J. Jobson, G. A. Woodell, and G. D. Hines, "Automated, on-board terrain analysis for precision landings," in *Proc. SPIE*, Apr. 2006, pp. 62460J-1–62460J-13.
[88] E. H. Land, "Recent advances in retinex theory and some implications for cortical computations: Color vision and the natural image," *Proc. Nat. Acad. Sci. USA*, vol. 80, pp. 5163–5169, Aug. 1983.
[89] B. K. P. Horn, "On lightness," MIT Artif. Intell. Memo. No. 295, Oct. 1973.
[90] A. Hurlbert, "Formal connections between lightness algorithms," *J. Opt. Soc. Amer. A*, vol. 3, no. 10, pp. 1684–1693, 1986.
[91] J. McCann, "Lessons learned from Mondrians applied to real images and color gamuts," in *Proc. Color Imag. Conf.*, 1999, pp. 1–8.
[92] B. Funt, F. Ciurea, and J. McCann, "Retinex in MATLAB," *J. Electron. Imag.*, vol. 13, no. 1, pp. 48–57, Jan. 2004.
[93] D. J. Jobson, Z.-U. Rahman, and G. A. Woodell, "Properties and performance of a center/surround retinex," *IEEE Trans. Image Process.*, vol. 6, no. 3, pp. 451–462, Mar. 1997.
[94] J. J. Daniel and W. A. Glenn, "Properties of a center/surround retinex: Part 2. Surround design," Nat. Aeronautics Space Admin., Washington, DC, USA, Tech. Rep. 110188, 1995, pp. 1–14.
[95] Z.-U. Rahman, D. J. Jobson, and G. A. Woodell, "Multi-scale retinex for color image enhancement," in *Proc. IEEE Int. Conf. Image Process.*, vol. 3. Sep. 1996, pp. 1003–1006.
[96] D. J. Jobson, Z.-U. Rahman, and G. A. Woodell, "A multiscale retinex for bridging the gap between color images and the human observation of scenes," *IEEE Trans. Image Process.*, vol. 6, no. 7, pp. 965–976, Jul. 1997.

[97] A. Moore, J. Allman, and R. M. Goodman, "A real-time neural system for color constancy," *IEEE Trans. Neural Netw.*, vol. 2, no. 2, pp. 237–247, Mar. 1991.

[98] A. B. Petro, C. Sbert, and J.-M. Morel, "Multiscale retinex," *Image Process. On Line*, vol. 4, pp. 71–88, Apr. 2014.

[99] W.-W. Hu, R.-G. Wang, S. Fang, and Q. Hu, "Retinex algorithm for image enhancement based on bilateral filtering," *J. Eng. Graph.*, vol. 31, no. 2, pp. 104–109, 2010.

[100] W. Yang, R. Wang, S. Fang, and X. Zhang, "Variable filter Retinex algorithm for foggy image enhancement," (in Chinese), *J. Comput.-Aided Design Comput. Graph.*, vol. 22, no. 6, pp. 965–971, Jul. 2010.

[101] R. C. Gonzalez and R. E. Woods, *Digital Image Processing*. Upper Saddle River, NJ, USA: Prentice-Hall, 2007.

[102] Y. Gao, L. Yun, J. Shi, F. Chen, and L. Lei, "Enhancement MSRCR algorithm of color fog image based on the adaptive scale," in *Proc. SPIE*, Apr. 2014, pp. 91591B-1–91591B-7.

[103] J.-Y. Kim, L.-S. Kim, and S.-H. Hwang, "An advanced contrast enhancement using partially overlapped sub-block histogram equalization," *IEEE Trans. Circuits Syst. Video Technol.*, vol. 11, no. 4, pp. 475–484, Apr. 2001.

[104] L. J. Wang and R. Zhu, "Image defogging algorithm of single color image based on wavelet transform and histogram equalization," *Appl. Math. Sci.*, vol. 7, no. 79, pp. 3913–3921, 2013.

[105] M. Kim and M. Chung, "Recursively separated and weighted histogram equalization for brightness preservation and contrast enhancement," *IEEE Trans. Consum. Electron.*, vol. 54, no. 3, pp. 1389–1397, Aug. 2008.

[106] T. K. Kim, J. K. Paik, and B. S. Kang, "Contrast enhancement system using spatially adaptive histogram equalization with temporal filtering," *IEEE Trans. Consum. Electron.*, vol. 44, no. 1, pp. 82–87, Feb. 1998.

[107] O. Patel, Y. P. S. Maravi, and S. Sharma, "A comparative study of histogram equalization based image enhancement techniques for brightness preservation and contrast enhancement," *Signal Image Process., Int. J.*, vol. 4, no. 5, pp. 11–25, 2013.

[108] K. Zuiderveld, "Contrast limited adaptive histogram equalization," in *Graphics gems IV* . San Diego, CA, USA: Academic, 1994, pp. 474–485.

[109] M.-J. Seow and V. K. Asari, "Ratio rule and homomorphic filter for enhancement of digital colour image," *Neurocomputing*, vol. 69, nos. 7–9, pp. 954–958, Mar. 2006.

[110] S. Dippel, M. Stahl, R. Wiemker, and T. Blaffert, "Multiscale contrast enhancement for radiographies: Laplacian pyramid versus fast wavelet transform," *IEEE Trans. Med. Imag.*, vol. 21, no. 4, pp. 343–353, Apr. 2002.

[111] C. Busch and E. Debes, "Wavelet transform for analyzing fog visibility," *IEEE Intell. Syst.*, vol. 13, no. 6, pp. 66–71, Nov./Dec. 1998.

[112] J. Jia and H. Yue, "A wavelet-based approach to improve foggy image clarity," in *Proc. IFAC World Congr.*, Aug. 2014, pp. 930–935.

[113] Z. Rong and W. L. Jun, "Improved wavelet transform algorithm for single image dehazing," *Optik-Int. J. Light Electron Opt.*, vol. 125, no. 13, pp. 3064–3066, Jul. 2014.

[114] Y. Yang, Z. Fu, X. Li, C. Shu, and X. Li, "A novel single image dehazing method," in *Proc. Int. Conf. Comput. Problem-Solving*, Oct. 2013, pp. 275–278.

[115] Z. Ma, J. Wen, Q. Liu, and G. Tuo, "Near-infrared and visible light image fusion algorithm for face recognition," *J. Modern Opt.*, vol. 62, no. 9, pp. 745–753, May 2015.

[116] P.-C. Zhou, F. Wang, H.-K. Zhang, and M.-G. Xue, "Camouflaged target detection based on visible and near infrared polarimetric imagery fusion," in *Proc. SPIE*, Aug. 2011, pp. 81940Y-1–81940Y-7.

[117] Z. Zhang, Y. Xu, J. Yang, X. Li, and D. Zhang, "A survey of sparse representation: Algorithms and applications," *IEEE Access*, vol. 3, no. 1, pp. 490–530, May 2015.

[118] C. O. Ancuti, C. Ancuti, and P. Bekaert, "Effective single image dehazing by fusion," in *Proc. IEEE Int. Conf. Image Process.*, Sep. 2010, pp. 3541–3544.

[119] C. O. Ancuti and C. Ancuti, "Single image dehazing by multi-scale fusion," *IEEE Trans. Image Process.*, vol. 22, no. 8, pp. 3271–3282, Aug. 2013.

[120] Y. Rao and L. Chen, "A survey of video enhancement techniques," *J. Inf. Hiding Multimedia Signal Process.*, vol. 3, no. 1, pp. 71–99, 2012.

[121] F. Guo, Z.-X. Cai, and B. Xie, "Video defogging algorithm based on fog theory," (in Chinese), *Acta Electron. Sinica*, vol. 39, no. 9, pp. 2019–2025, Sep. 2011.

[122] A. S and A. Ali, "A novel method for video dehazing by multi-scale fusion," *Int. J. Sci. Eng. Technol. Res.*, vol. 3, no. 24, pp. 4808–4813, Sep. 2014.

[123] C. Ramya and S. S. Rani, "A novel method for the contrast enhancement of fog degraded video sequences," *Int. J. Comput. Appl.*, vol. 54, no. 13, pp. 1–5, Sep. 2012.

[124] I. Yoon, S. Kim, D. Kim, M. H. Hayes, and J. Paik, "Adaptive defogging with color correction in the HSV color space for consumer surveillance system," *IEEE Trans. Consum. Electron.*, vol. 58, no. 1, pp. 111–116, Feb. 2012.

[125] A. Chambolle, "An algorithm for total variation minimization and applications," *J. Math. Imag. Vis.*, vol. 20, nos. 1–2, pp. 89–97, 2004.

[126] B. Xie, F. Guo, and Z. Cai, "Universal strategy for surveillance video defogging," *Opt. Eng.*, vol. 51, no. 10, pp. 101703-1–101703-7, 2012.

[127] Z.-L. Ma, J. Wen, and L.-L. Hao, "Video image defogging algorithm for surface ship scenes," (in Chinese), *Syst. Eng. Electron.*, vol. 36, no. 9, pp. 1860–1867, Sep. 2014.

[128] Y. Zhang, J.-W. Zhang, G.-Q. Yang, and L. Liang, "Video de-hazing using spatial-temporal coherence optimization," *Appl. Res. Comput.*, vol. 28, no. 10, pp. 3983–3985, Oct. 2011.

[129] Z. Wang, A. C. Bovik, H. R. Sheikh, and E. P. Simoncelli, "Image quality assessment: From error visibility to structural similarity," *IEEE Trans. Image Process.*, vol. 13, no. 4, pp. 600–612, Apr. 2004.

[130] M. Carnec, P. Le Callet, and D. Barba, "Objective quality assessment of color images based on a generic perceptual reduced reference," *Signal Process., Image Commun.*, vol. 23, no. 4, pp. 239–256, Apr. 2008.

[131] H. R. Sheikh, A. C. Bovik, and L. Cormack, "No-reference quality assessment using natural scene statistics: JPEG2000," *IEEE Trans. Image Process.*, vol. 14, no. 1, pp. 1918–1927, Nov. 2005.

[132] A. M. Rohaly, J. Libert, P. Corriveau, and A. Webster. (2000). *Final Report From the Video Quality Experts Group on the Validation of Objective Models of Video Quality Assessment*. [Online]. Available: www.vqeg.org

[133] H. Tamura, S. Mori, and T. Yamawaki, "Textural features corresponding to visual perception," *IEEE Trans. Syst., Man, Cybern.*, vol. 8, no. 6, pp. 460–473, Jun. 1978.

[134] Z. Chen, T. Jiang, and Y. Tian, "Quality assessment for comparing image enhancement algorithms," in *Proc. IEEE Conf. Comput. Vis. Pattern Recognit. (CVPR)*, Jun. 2014, pp. 3003–3010.

[135] K. B. Gibson and T. Q. Nguyen, "A no-reference perceptual based contrast enhancement metric for ocean scenes in fog," *IEEE Trans. Image Process.*, vol. 22, no. 10, pp. 3982–3993, Oct. 2013.

[136] N. Hautière, J.-P. Tarel, D. Aubert, and É. Dumont, "Blind contrast enhancement assessment by gradient ratioing at visible edges," *Image Anal. Stereol. J.*, vol. 27, no. 2, pp. 87–95, Jun. 2008.

[137] T. L. Economopoulos, P. A. Asvestas, and G. K. Matsopoulos, "Contrast enhancement of images using partitioned iterated function systems," *Image Vis. Comput.*, vol. 28, no. 1, pp. 45–54, 2010.

[138] N. Hautière and D. Aubert, "Visible edges thresholding: A HVS based approach," in *Proc. Int. Conf. Pattern Recognit.*, vol. 2. 2006, pp. 155–158.

[139] M. Nixon and A. Aguado, *Feature Extraction & Image Processing for Computer Vision*. Beijing, China: Publishing House of Electronics Industry, 2013.

[140] Z. Wang and A. C. Bovik, "A universal image quality index," *IEEE Signal Process. Lett.*, vol. 9, no. 3, pp. 81–84, Mar. 2002.

[141] K. He and J. Sun. (2015). "Fast Guided Filter." [Online]. Available: http://arxiv.org/abs/1505.00996

YONG XU was born in Sichuan, China, in 1972. He received the Ph.D. degree in pattern recognition and intelligence system from the Nanjing University of Science and Technology, in 2005. He is currently with the Shenzhen Graduate School, Harbin Institute of Technology. His current interests include pattern recognition, biometrics, machine learning, and video analysis.

JIE WEN received the M.S. degree from Harbin Engineering University, China, in 2015. He is currently pursuing the Ph.D. degree in computer science and technology with the Shenzhen Graduate School, Harbin Institute of Technology, Shenzhen, China. His research interests include, image and video enhancement, pattern recognition, and machine learning.

LUNKE FEI received the B.S. and M.S. degrees in computer science and technology from East China Jiaotong University, China, in 2004 and 2007, respectively. He is currently pursuing the Ph.D. degree in computer science and technology with the Shenzhen Graduate School, Harbin Institute of Technology, Shenzhen, China. His current research interests include pattern recognition and biometrics.

ZHENG ZHANG received the B.S. degree from the Henan University of Science and Technology, in 2012, and the M.S. degree from the Shenzhen Graduate School, Harbin Institute of Technology (HIT), Shenzhen, China, in 2012 and 2014, respectively. He is currently pursuing the Ph.D. degree in computer science and technology with the Shenzhen Graduate School, HIT. His current research interests include pattern recognition, machine learning, and computer vision.